

Contents lists available at ScienceDirect

Chemosphere

journal homepage: www.elsevier.com/locate/chemosphere



Review

A review on MXene-based nanomaterials as adsorbents in aqueous solution



Minjung Jeon a , Byung-Moon Jun a , Sewoon Kim a , Min Jang b , Chang Min Park c , Shane A. Snyder $^{d,\,e}$, Yeomin Yoon $^{a,\,*}$

- ^a Department of Civil and Environmental Engineering, University of South Carolina, Columbia, 300 Main Street, SC, 29208, USA
- ^b Department of Environmental Engineering, Kwangwoon University, 447-1 Wolgye-Dong Nowon-Gu, Seoul, Republic of Korea
- ^c Department of Environmental Engineering, Kyungpook National University, 80 Daehak-ro, Buk-gu, Daegu, 41566, Republic of Korea
- ^d School of Civil & Environmental Engineering, Nanyang Technological University, 1 Cleantech Loop, 637141, Singapore
- ^e Department of Chemical and Environmental Engineering, University of Arizona, Tucson, AZ, 85721, USA

HIGHLIGHTS

- Removal of inorganic and organic contaminants by MXene-based nanomaterials was reviewed.
- Valuable information was provided for applications of MXene-based nanomaterials in wastewater treatment.
- Areas of future research for the removal of various contaminants in MXene-based nanomaterials were suggested.

ARTICLE INFO

Article history:
Received 15 June 2020
Received in revised form
16 July 2020
Accepted 17 July 2020
Available online 24 July 2020

Handling Editor: Xiangru Zhang

Keywords: Adsorption MXene nanoadsorbents Heavy metal Dye Water/wastewater treatment

ABSTRACT

Environmental pollution has intensified and accelerated due to a steady increase in the number of industries, and finding methods to remove hazardous contaminants, which can be typically divided into inorganic and organic compounds, have become inevitable. One of the widely used water treatment technologies is adsorption and various kinds of adsorbents for the removal of inorganic and organic contaminants from water have been discovered. Recently, MXene, as an emerging nanomaterial, has gained rapid attention owing to its unique characteristics and various applicability. Particularly, in the area of adsorptive application, MXene and MXene-based adsorbents have shown great potential in a large number of studies. In this regard, a comprehensive understanding of the adsorptive behavior of MXene-based nanomaterials is necessary in order to explain how they remove inorganic and organic contaminants in water. Adsorption by MXene-based adsorbents tends to be highly influenced by not only the physicochemical properties of these adsorbents but also water quality, such as pH value, temperature, background ion, and natural organic matter. Therefore, in this review paper, the effect of various water quality on the adsorption of inorganic and organic contaminants by various types of MXene and MXene-based adsorbents is explored. Furthermore, this review also covers general trends in the synthesis of MXene and regeneration of MXene-based adsorbents in order to assess their stability.

© 2020 Elsevier Ltd. All rights reserved.

Contents

1.	Introd	luction	2
2.	Fabric	cation and characteristics of MXene	3
		General fabrication process of MXene	
		Etching method	
		2.2.1 HF	
		222 In situ HF	

E-mail address: yoony@cec.sc.edu (Y. Yoon).

^{*} Corresponding author.

	2.3.		tion method	
		2.3.1. In	ntercalation	. 5
		2.3.2. So	onication	. 5
3.	Remo	val of inorg	ganic contaminants by MXene nanomaterials	. 5
	3.1.	Effects of	contaminant and MXene properties	. 5
	3.2.		water quality	
		3.2.1. pl	н	. 9
		3.2.2. B	ackground ions and NOM	. 9
		3.2.3. To	emperature	10
4.	Remo	val of organ	nic contaminants by MXene nanomaterials	10
	4.1.	Effects of	contaminant and MXene properties	10
	4.2.	Effects of	water quality	12
			н	
		4.2.2. B	ackground ions and NOM	13
		4.2.3. To	emperature	13
5.	Regen	eration of l	MXene nanomaterials	14
6.	Concl	usions and	areas of future study	14
	Decla	ration of co	ompeting interest	16
	Ackno	wledgeme	nts	16
	Refere	ences		16

1. Introduction

Various contaminants have been discharged into water inadequately treated and cause severe environmental pollution and harm to human health, as rapid developments in industrialization continue (Jasper et al., 2017). The contaminants can generally be divided into two groups: organic and inorganic. Among the organic contaminants are typically dye compounds such as methylene blue, which are discharged generally by factories manufacturing textile, paint, paper, etc. (Karacetin et al., 2014). For inorganic contaminants, heavy metal ions and radionuclides are the dominant pollutants in water (Zhang et al., 2018). They have adverse effects on living things and the natural environment in general due to their toxicity and carcinogenicity. Since some of them can be bioaccumulated, the damage they cause in living organisms could be more severe than that caused by other pollutants, which cannot be bioaccumulated (Berrios et al., 2012; Fu et al., 2018; Karaçetin et al., 2014). Thus, the implementation of appropriate treatment methods for the removal of these contaminants has been regarded as one of the main determinants of the prosperity of industries in the long

To date various techniques have been used for the removal of several organic and inorganic pollutants from water, such as coagulation (Fu and Wang, 2011; Moghaddam et al., 2010), ion exchange (Dabrowski et al., 2004; Fu and Wang, 2011), sorption (Fu and Wang, 2011; Gong et al., 2007), membrane filtration (Blöcher et al., 2003; Fu and Wang, 2011), chemical precipitation (Fu and Wang, 2011; Fu et al., 2012), sonodegradation (Ertugay and Acar, 2014; Wang et al., 2010b), and photocatalytic oxidation (Ertugay and Acar, 2014; Sakthivel et al., 2003). Among these techniques, adsorption is one of the most widely used due to its attractive characteristics such as cost-effectiveness, simplicity, and practicality (Burakov et al., 2018; Wu et al., 2019). In addition, employing adsorbents for the removal of environmental pollutants prevents the formation of secondary pollutants since the adsorbents adsorb the contaminants, not react with them (Wu et al., 2019; Zhang et al., 2018). There are several conventional adsorbents, such as granular or powdered activated carbon (Oguz and Keskinler, 2005), kaolin, and chitosan (Wang et al., 2010a; Zhu et al., 2010), to name a few, which are widely used due to their high porosity and large surface area. In recent years, two-dimensional (2D) nanomaterials have attracted great attention as emerging adsorbents for the effective removal of various environmental contaminants due to their distinct properties, which can result in significant adsorptive remediation (Fu et al., 2018; Wu et al., 2019). The unique properties of 2D nanomaterials, such as carbon-based nanomaterials, have increased the tendency to employ nanomaterial-based adsorbents for the treatment of inorganic and organic pollutants in water (Atkovska et al., 2018; Liu et al., 2017b). Compared to the large and bulky formation of the conventional adsorbents, nanomaterialbased adsorbents often possess thin structures, large specific surface area, and abundant functional sites (Novoselov et al., 2004; Zhang et al., 2018). Since it is important for adsorbents to display great interaction with adsorbates and have large surface area for better performance, nanomaterials are regarded as having the potential to treat not only organic but also inorganic adsorbates (Tan et al., 2015; Yang et al., 2019).

Recently, an emerging class of 2D nanomaterials from a family of transition metal carbide or nitrate materials, known as MXene, has aroused tremendous interest in various fields. Due to their properties such as environmental-friendly characteristics, large surface area, high chemical stability, thermal/electrical conductivity, and hydrophilicity, MXenes can be employed as suitable materials in various applications including lithium-ion battery (Naguib et al., 2012a), hydrogen storage (Hu et al., 2013), semiconductor (Gao et al., 2016), supercapacitor (Zhu et al., 2016), and environmental applications (Ciou et al., 2019; Liu et al., 2018a; Peng et al., 2014).

In particular, the possible environmental applications include adsorption, photocatalysis, and membrane filtration to remove contaminants, and adsorption using MXenes and MXene-based materials as adsorbents for the removal of organic and inorganic pollutants from water has been widely studied (Guo et al., 2016a, 2016b; Rasool et al., 2017). Since MXene-based adsorbents can adsorb various environmental pollutants owing to their unique structures (Ying et al., 2015), it is important to fully understand the adsorption mechanisms and interaction between pollutants and the adsorbents. Additionally, the adsorption process of both kinds of pollutants in water is highly affected by not only the adsorbents' properties but also by the water quality conditions such as temperature, pH, and the presence of natural organic matter (NOM). In this regard, it is critical to evaluate the influence of the water quality properties on the adsorption performance, leading to better

understanding of the adsorbents and ultimately the removal of pollutants.

In this review paper, the main purpose is to deliver the overall knowledge of MXene and MXene-based nanomaterials and their properties and to provide an overview of the adsorptive applications of various functionalized MXene-based nanomaterials as novel adsorbents for the removal of inorganic and organic pollutants from water. Although a few review studies have already covered the use of MXenes as adsorbents in water treatment (Jun et al., 2018; Rasool et al., 2019; Zhang et al., 2018), their adsorptive application with regard to their water quality properties, including pH, background ions and NOM, and temperature, has not been thoroughly explored yet. Additionally, since one of the advantages of adsorbents is that they can be recycled after some proper regenerating processes, regeneration methods and adsorptive performance after regeneration of the used adsorbents are included in this review to clarify the stability and economic feasibility of MXenes and MXene-based nanomaterials from various literature.

2. Fabrication and characteristics of MXene

2.1. General fabrication process of MXene

MXenes can be synthesized from MAX phases, a family of ternary carbides and nitrides, as the pristine formula, which consists of M, A, and X, representing an early transition metal (Ti, Nb, V, Ta, etc.), an A-group element from groups 13 and 14 (such as Al or Si), and C and/or N, respectively (Lei et al., 2015). Generally, the fabrication process includes etching and delamination. By etching A layers in MAX phases, which is probable owing to A layers being relatively weakly bound with M elements compared to M-X bonds, the general formation of MAX phases, $M_{n+1}AX_n$ (n = 1, 2 or 3), turns into the multilayered $M_{n+1}X_n$ (Chang et al., 2013). Following the etching step, delamination is also conducted to yield single-layered MXene by enlarging the space in between the layers with intercalants and sonicating the result of the intercalation if the specific size of flakes or concentration is required (Alhabeb et al., 2017).

The general history of fabrication of MXenes has been thoroughly covered by a few studies (Alhabeb et al., 2017; Anasori et al., 2017; Naguib et al., 2012a, 2014), and, according to them, fabrication of MXene has gone through a series of development beginning from 2011 when for the first time MXene was discovered by scientists at Drexel University (Naguib et al., 2011). The reported etching method was conducted with 50% concentrated hydrofluoric acid (HF) solution, which is one of the typical and effective etchants used even till today (Alhabeb et al., 2017). Following their discovery, other types of multilayered MXenes with different elements of MAX phases were synthesized by the wet chemical etching technique. Intercalation, which is a part of the delamination step, was presented afterwards in order to produce singlelayered MXenes by introducing large organic compounds, such as urea, hydrazine monohydrate, dimethyl sulfoxide, isopropylamine, and tetrabutylammonium hydroxide, in between the layers (Mashtalir et al., 2013, 2015; Naguib et al., 2015). From 2014, new approaches to etching were reported, which did not use HF solution but ammonium bifluoride (Halim et al., 2014) or HCl with LiF (Ghidiu et al., 2014; Lipatov et al., 2016) in order to satisfy the high demand for etchants less dangerous than HF solution. Furthermore, to date, the application of MXene has been expanded to electronic fields such as in antennas for wireless communication and nanowire electrodes for flexible organic solar cells employing its unique conductivity, hydrophilicity, and thin structure (Sarycheva et al., 2018; Tang et al., 2019). Fig. 1 shows the overall timeline of the development of MXene and MXene-based materials, including from the discovery in 2011 to the recent electronic applications.

2.2. Etching method

The purpose of etching in the fabrication process is to successfully exfoliate A layers from MAX phases (Naguib and Gogotsi, 2015). In Fig. 2a, the schematic and atomic model of well-etched Ti₃C₂T_x and its scanning electron microscopy (SEM) image are shown. There are generally two etching methods: HF method and in situ HF method (Alhabeb et al., 2017). HF method involves literally using various concentrations of HF solution as etchants. In situ HF method, on the other hand, does not utilize HF solution directly, but uses HF-containing or HF-forming etchants. In situ HF method was invented because high concentrations of HF solution could expose people to considerable risks due to its hazards (Feng et al., 2017). It was also expected that the etchants used in in situ HF method could act as intercalants as well (Halim et al., 2014). Exceptionally, there is another way to etch A layers without employing a fluoride-containing etchant, but by using other reagents, such as NaOH and H2SO4, although much research has not been conducted in that regard (Xie et al., 2014). Depending on what kinds and concentration of etchants are used, the further process, as discussed later in the section on delamination, could be influenced accordingly. To conduct a successful wet chemical etching process, appropriate etchants and synthesis conditions are necessary, and the characteristics of the etched materials vary depending on them (Alhabeb et al., 2017; Hong Ng et al., 2017; Lei et al., 2015; Lipatov et al., 2016).

2.2.1. HF

HF solution is one of the most common etchants used to etch A layers in the parent MAX phases (Alhabeb et al., 2017; Chang et al., 2013; Hong Ng et al., 2017). Fig. 2b briefly describes the process of etching of a MAX phase using HF solution. By immersing the MAX phase in HF solution, the A element (Al being a typical example) reacts with fluorine from the etchant and eventually becomes etched in the MAX phases to form aluminum fluoride (AlF₃) (Lei et al., 2015). HF also reacts with multilayered MXene, thus having MXene consist of F on its surface as part of its functional groups (Hong Ng et al., 2017). Etching conditions, including the concentration of HF solution, temperature, and duration of immersion, greatly affect the resulting MXene, which is the reason why finding an optimum combination of the etching conditions is necessary for better performance of the resultant (Lei et al., 2015; Lipatov et al., 2016; Naguib and Gogotsi, 2015). Concentration of the etchant varies from 5 to 50 wt % HF and so does exposure time vary according to the concentration, from 5 to 24 h. The influence of individual etching conditions on the result of the etching process can be confirmed by SEM, energy dispersive X-ray (EDX), and powder X-ray diffraction (XRD) (Alhabeb et al., 2017; Chang et al., 2013; Ying et al., 2015).

By varying the concentration of HF solution, MXenes with different morphology can be fabricated. It was reported that more sophisticatedly etched $\rm Ti_3C_2T_x$ can be synthesized by using HF solutions at higher concentrations (Alhabeb et al., 2017). The etching performance of three different concentrations (5, 10, and 30 wt %) of HF etchants were compared and it was confirmed, through their SEM images, that the resulting MXene of 30 wt % HF solution has a well-etched, almost accordion-like structure. Compared to the 30 wt % HF, the resulting morphology of the MXenes of the 10 wt % and 5 wt % HF solution were less open, and also hardly expanded in case of the 5 wt %. Although it was observed by XRD and EDX that all three different concentrations of the etchant played their roles as reagents for the exfoliation of the A layer effectively, the highest concentration of HF was able to synthesize MXene with a distinct

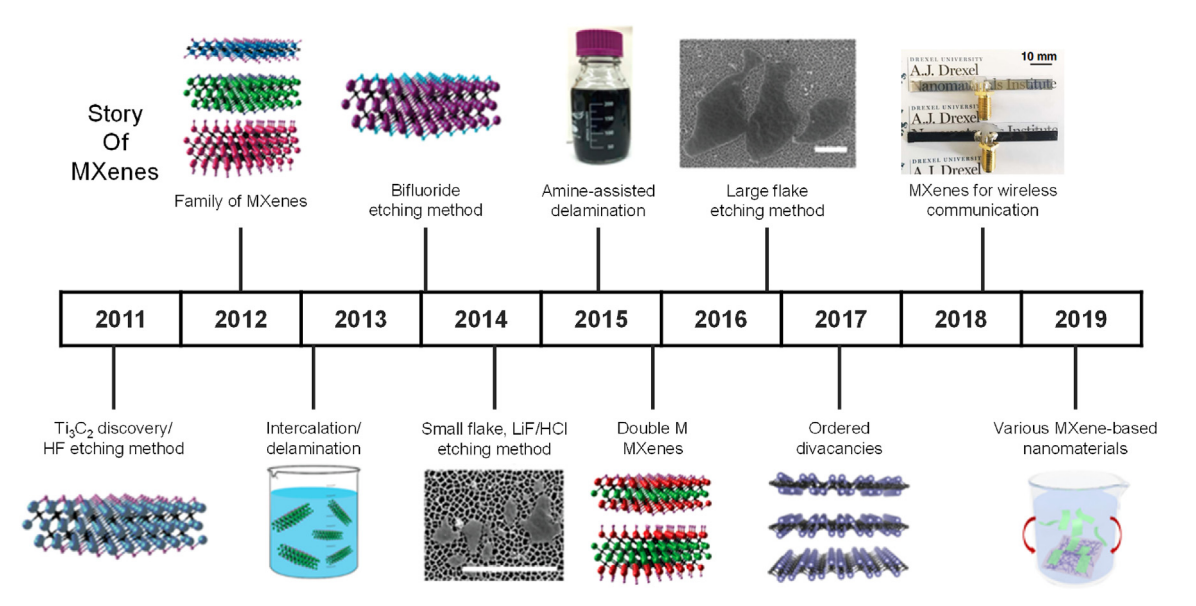


Fig. 1. Timeline of MXenes: from Ti₃C₂ discovery to the current development (Al-Hamadani et al., 2020; Alhabeb et al., 2017).

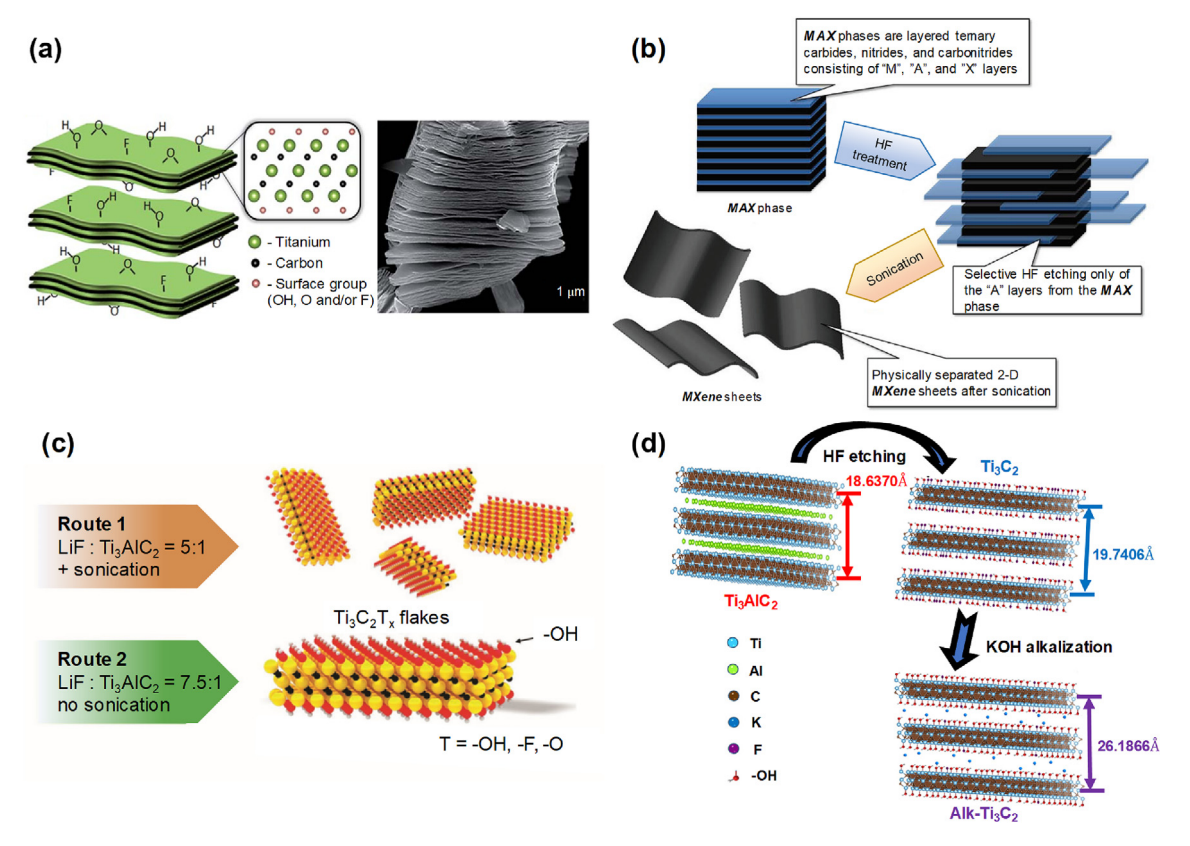


Fig. 2. (a) Schematic of (a) Ti₃C₂T_x layered structure with a side view atomic model of a single sheet and SEM image of a Ti₃C₂T_x particle (Mashtalir et al., 2014), (b) the exfoliation of MAX phases and formation of MXenes (Naguib et al., 2012b), (c) structures of Ti₃C₂T_x with summary of routes 1 and 2 (Lipatov et al., 2016), and (d) structural illustrations of the parental Ti₃AlC₂ MAX phase and the post-etching MXene before and after alkalization treatment (Zhu et al., 2017).

accordion-like structure and larger surface area (Alhabeb et al., 2017). The duration of immersion of the MAX phase in HF solution also affects the result of the etching process (Chang et al., 2013). In this study, ${\rm Ti}_3{\rm AlC}_2$ powders were etched by 40 wt % HF solution at room temperature after being ball-milled for 5 h and sintered at 1350 °C for 2 h. As the time of reaction increased, it was

found that the layers of etched MXene became thinner and, accordingly, the space between layers was enlarged by exfoliating the A-group. The XRD patterns of the pristine Ti₃AlC₂ and the HF-treated resultant showed a weakening trend in the diffraction peaks of the former as the duration of immersion prolonged from 4 to 20 h. On the other hand, the peaks of the latter were shown

clearly, and no peak changes could be noted after 2 h, which could imply that the resulting multilayered MXene likely possessed thinner-layered morphology due to the extended reaction time (Chang et al., 2013).

2.2.2. In situ HF

In order to avoid the use of high concentrations of HF solution due to the high risks attributed to the critical corrosiveness of HF. in situ HF etching method was discovered as a safer way to synthesize MXene (Halim et al., 2014). The reagents used in this method generally contain HF or form HF through reaction, thus employing a similar effect to HF method to exfoliate A layers from MAX phases. Some of the typical etchants that are used for in situ HF method are ammonium bifluoride, ammonium fluoride, and LiF/HCl (Ghidiu et al., 2014; Halim et al., 2014; Lipatov et al., 2016; Shahzad et al., 2019a; Zhang et al., 2019a). Additional advantages other than less hazards compared to HF are that etching and intercalation, as we would see later, could be conducted at the same time and sonication is not compulsory in the process of fabrication (Halim et al., 2014; Hong Ng et al., 2017; Naguib et al., 2015). Also, other newly invented etchants, such as FeF₃/HCl (Wang et al., 2017b), in which LiF is replaced with FeF₃, are consistently being investigated.

In order to simplify the etching process, including carrying out etching and intercalation as one step, 2D thin Ti_3C_2 films was fabricated using ammonium bifluoride as an etchant (Halim et al., 2014). By immersing Ti_3AlC_2 in the etchant, it was found that it is possible for Al to be selectively etched by forming (NH₄)₃AlF₆, and from their X-ray photoelectron spectroscopy (XPS) analysis of nitrogen, they concluded that NH₃ or NH₄⁺ could be intercalated in between the etched phases, thus making the interlayers more spacious. They also discovered that the c lattice parameter, confirmed by XRD, of $Ti_3C_2T_x$ etched by ammonium bifluoride is 2.47 nm while that of the same $Ti_3C_2T_x$ etched by HF is 1.98 nm, showing almost a 25% increase in the c lattice parameter. They concluded from this result that intercalation and etching were successfully performed at the same time (Halim et al., 2014).

LiF/HCl is also one of the widely used in situ HF etchants and the concentrations of LiF and HCl vary depending on the desired condition of MXene (Ghidiu et al., 2014; Lipatov et al., 2016; Zhang et al., 2019c). By using 5 M LiF and 6 M HCl to etch Al in Ti₃AlC₂, the A layers were well etched, indicated by XRD analysis showing absence of peaks belonging to Ti₃AlC₂. Comparing the lattice parameters of c, the one of MXene etched by LiF/HCl was 2.8 nm while that of the one etched by HF is 2.0 nm. Furthermore, the c lattice of hydrated MXene produced by LiF/HCl was 4.0 nm, which can be assumed to be swollen owing to the intercalation of H₂O and the cations in the solution. It was also reported that this LiF/HCl method can reduce the time of synthesis of MXene by shortening the duration of sonication step from 4 h to 30-60 min (Ghidiu et al., 2014). Concentrations of LiF higher than 5 M and of HCl higher than 6 M can be used to minimize the necessity of the sonication step (Lipatov et al., 2016). Schematic structures of MXene etched with different concentrations of LiF are shown in Fig. 2c.

2.3. Delamination method

After etching, delamination follows, which is accomplished through intercalation and sonication (Alhabeb et al., 2017). Intercalation is the introduction of various ions or molecules between layers of etched MXene, thus enlarging the interspace between the layers, which results in an increase in the surface area and even the delamination of the layers into a 2D structure (Guo et al., 2015; Mashtalir et al., 2013; Naguib et al., 2015). As mentioned earlier, there are two steps for delaminating layered MXene, which are intercalation and sonication. Various intercalants can be used, such

as large organic compounds, various ions from the etchant, and etc. The next step is sonication and the purpose of this process is to produce the desired size of flakes or concentration of 2D MXene by sonicating intercalated MXene. In other words, sonication could be optional if there is no requirement of a particular concentration or flake size for the resulting MXene (Alhabeb et al., 2017; Mashtalir et al., 2013; Naguib et al., 2015).

2.3.1. Intercalation

Intercalation is conducted after etching to accommodate ions or organic compounds in order to expand the space in between the layers of un-delaminated MXene, considered as a pre-treatment before sonication, which ultimately leads to the delamination of the layers (Alhabeb et al., 2017; Mashtalir et al., 2013). Generally, after HF etching, the -OH and -F functional groups first become part of the surface of the resulting multilayered MXene (Lukatskaya et al., 2013). Then, other cations from the intercalants could replace some of the initial functional groups, which may increase the selectivity of the resultant for the target pollutants after the intercalation process (Peng et al., 2014). Some of the possible intercalants are dimethyl sulfoxide and tetraalkylammonium compounds, such as tetrabutylammonium hydroxide and tetramethylammonium hydroxide (Ma and Sasaki, 2015; Mashtalir et al., 2013). LiF/HCl, which is one of the etchants used in in situ HF method, could play two roles as an etchant and an intercalant owing to the high likability of Li⁺ ions intercalated in between layers (Ghidiu et al., 2014; Lipatov et al., 2016). Ammonium bifluoride may also have a similar effect as LiF/HCl, which could be attributed to the intercalation of the ammonia species, NH₃ and NH[±] (Halim et al., 2014). Water molecules could sometimes be one of the intercalated species which greatly expand the c lattice parameter (Ghidiu et al., 2014; Wang et al., 2017a). Up until now, research on intercalation effect and potential intercalants, such as alkaline intercalant (Wang et al., 2017b; Zhu et al., 2017), has been steadily conducted. Fig. 2d illustrates the synthesis process of $Ti_3C_2T_x$ intercalated by an alkaline solution.

2.3.2. Sonication

Sonication is considered the last step of the fabrication of MXene and its aim is to manage the size of flakes and concentration of MXene (Alhabeb et al., 2017). In fact, there are several ways to control the size of the flakes, one of which involves using centrifugation to separate larger-sized MXene particles from the solution containing smaller sizes of MXene in colloidal state (Ghidiu et al., 2014; Lipatov et al., 2016; Wang et al., 2017b). Another method is to reduce the size of MXene by sonication before centrifugation so that the un-delaminated particles could be exfoliated, thereby increasing the concentration of colloidal MXene in the solution (Backes et al., 2017; Mashtalir et al., 2015). Although the size and concentration of MXene can be controlled by centrifugation. centrifugation alone is considered a limited option, and controlling the concentration and size by centrifugation after sonication is more effective for various possible applications since it yields a higher concentration or smaller flakes of MXene (Alhabeb et al., 2017).

3. Removal of inorganic contaminants by MXene nanomaterials

3.1. Effects of contaminant and MXene properties

The most common inorganic contaminants in water that can be removed by MXene-based nanomaterials are heavy metals and radionuclides (Zhang et al., 2018). MXene can be electrostatically charged and the surface charge of MXene is attributed to functional

groups on the surface (Naguib et al., 2012b). During etching and intercalation, various functional groups are formed on the surface of MXene, such as -O, -F, and -OH. A wide variety of functional groups which support adsorption reaction are formulated by etchants and intercalants (Mu et al., 2018; Peng et al., 2014). In other words, they could electrostatically interact with opposite charges from target compounds in water. Also, the charge on MXene depends on the pH of the solution due to protonation by hydrogen ions, MXene could adsorb negatively or positively charged targets depending on its charge (Khan et al., 2019; Mu et al., 2018; Shahzad et al., 2017). Due to their electrostatic property, various ions of heavy metals and radionuclides could be removed by MXene since they are oppositely charged to the MXene functional groups. Thus, there is electrostatic interaction between MXene and inorganic contaminants which is the main adsorption mechanism of MXene (Ying et al., 2015). Fig. 3 describes, with the aid of schematic diagrams, the adsorption of inorganic contaminants by MXene. Although electrostatic interaction is the dominant mechanism for the removal of inorganic pollutants, other mechanisms, such as ion exchange (Peng et al., 2014; Shahzad et al., 2017; Wang et al., 2016), and some factors, such as specific surface area, pH, and temperature, also greatly influence the adsorption process. Information regarding adsorptive removal of selected inorganic contaminants by MXene nanomaterials is summarized in Table 1.

Heavy metal adsorption of Cr(VI) using 2D $Ti_3C_2T_x$ MXene, which was etched by HF solutions of different concentrations (10, 25, and 50 wt %) and sonicated to exfoliate the respective layers, was carried out (Ying et al., 2015). Confirmed by Brunauer–Emmett–Teller (BET) results, the $Ti_3C_2T_x$ -10% nanosheets turned out to have 57 m² g⁻¹, the highest specific surface area among the fabricated MXenes used in this study, and pore volume

of 0.11 cm³ g⁻¹. Accordingly, the highest adsorption capacity of 250 mg g⁻¹ was achieved by the MXene using 10 wt % of HF solution, whereas the corresponding values for the other concentrations were slightly less. Due to the positive surface charge of Ti₃C₂T_x below a pH of 2, Cr ions in the form of $Cr_2O_7^{2-}$ can be removed from water as a result of the electrostatic interaction between the two charges. Additionally, through the adsorption, Cr(VI) was reduced to Cr(III) during adsorption. Cr(VI) can be reduced to Cr(III) in the presence of H⁺ ions and electrons to produce water molecules. Since MXene plays the role of electron donors, providing the adsorbed $Cr_2O_7^{2-}$ electrons, Cr(VI) is reduced, thus leading to a reduction in the hazards associated with Cr. MXene is not only effective in the reduction of Cr, but also Fe, Mn, and Au, in the forms of K₃[Fe(CN)₆], KMnO₄, and NaAuCl₄, respectively (Ying et al., 2015). Other studies on heavy metal adsorption by MXene have been conducted and most agree that the target contaminants are oppositely charged to the synthesized MXene and can interact electrostatically, thus enabling the adsorption process (Fard et al., 2017; Li et al., 2019; Shahzad et al., 2019a; Wang et al., 2017a).

Another example of heavy metal adsorption is the use of alkintercalated MXene $(Ti_3C_2(OH/ONa)_xF_{2-x})$ to remove Pb(II) in water in 5% NaOH solution for the intercalation of Na ions (Peng et al., 2014). By XRD and EDX analysis, it was confirmed that Na ions were successfully intercalated, and they expanded the space between layers, thus increasing the diffusion rate of the area which could react with Pb(II) ions. The obtained adsorption capacity was up to 140 mg g⁻¹, which is considered high compared to the capacities of other conventional Pb(II) adsorbents. Also, the alk-MXene attained equilibrium in 120 s, and this could be attributed to its ability to react extraordinarily with Pb(II) because of its distinct formation. The main mechanism used in this study was ion exchange, assumed

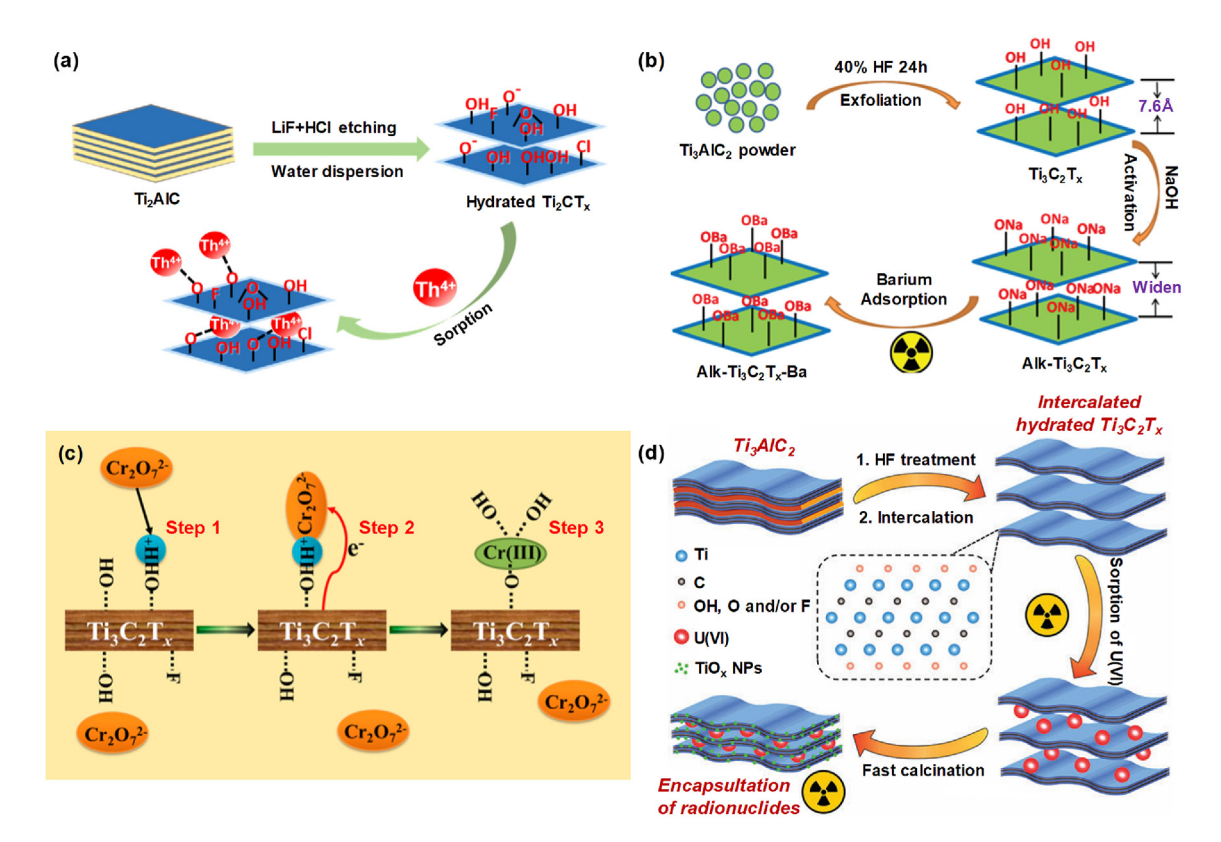


Fig. 3. (a) Schematic diagram of (a) thorium sorption onto Ti₂CT_x MXene (Li et al., 2019), (b) the adsorption of radioactive barium ions (Mu et al., 2018), (c) the removal mechanism of Cr(VI) by the Ti₃C₂T_x nanosheets (Ying et al., 2015), and (d) hydrated intercalation synthesis strategy of Ti₃C₂T_x MXene for efficient U(VI) uptake and imprisonment (Wang et al., 2017a).

 Table 1

 Summary of adsorptive removal of selected inorganic contaminants by MXene nanomaterials.

MXene	Species	$C_0 \text{ (mg L}^{-1}\text{)}$	Experimental condition	$q_{\rm m}~({\rm mg~g^{-1}})$	Main finding	Ref.
Γi ₃ C ₂ T _x	Ва	1-55	pH 3-9	9.3	The maximum adsorption capacity at	Fard et al. (2017)
			temp. = 298 K		$Ba = 55 \text{ mg L}^{-1} \text{ is 9.3 mg g}^{-1}$, which is much greater	
	_		synthetic water		value than those of other adsorbents.	
$Ti_3C_2T_x$	Cu	25	pH 2-6	86.5	Compared to a commercial activated carbon, the	Shahzad et al. (2017)
			temp. = 293–318 K		adsorption capacity of $Ti_3C_2T_x$ was nearly three	
ъ с т	U	100	synthetic water pH 5	214	times higher. Owing to the flexibility and large interlayer space,	Wang et al. (2017a)
Ti ₃ C ₂ T _x	U	100	рп 5 temp. = 293 K	214	the adsorption of U(VI) on hydrated $Ti_3C_2T_x$ was	Wallg et al. (2017a)
			synthetic water		significantly enhanced, compared to dry $Ti_3C_2T_x$.	
Magnetic Ti ₃ C ₂ T _x	Hg	25-1000	pH 2-9	1128	Magnetic $Ti_3C_2T_x$ has much better maximum $Hg(II)$	Shahzad et al. (2018)
magnetic 113e21x	8	25 1000	temp. = 288–318 K	1120	adsorption capacity than other two dimensional	briandia et un (2010)
			synthetic water		nanocomposite and nano-materials.	
Fi ₃ C ₂ (OH) _{0.8} F _{1.2}	Cr	10	pH 3-6	62	MXene which is chemically exfoliated in solutions	Zou et al. (2016)
			temp. = 298 K		having F ions consequently has the surface covered	
			synthetic water		with F groups	
odium alginate/Ti ₃ C ₂ T _x		0-10 mM	pH 1-7	87.6	By having abundant adsorption sites, the MXene/	Dong et al. (2019b)
	Pb		temp. = 298–333 K	383	alginate composite was able to achieve high	
			synthetic water		adsorption capacity of selected inorganic	
CT buildings of	TL/II/	F 100	-II 1 2 F	212	compounds and reach equilibrium in 15 min.	Li at al (2010)
Ti ₂ CT _x -hydrated	Th(IV)	5-180	pH 1–3.5 temp. = 282–312 K	213	Inner-sphere complexation from strong attraction between Ti–OH and Th(IV) is the mechanism for	Li et al. (2019)
			synthetic water		removal of Th(IV) by Ti_2CT_x in water.	
MX-SA _{2:20}	Hg	25-994	pH 0-11	365	Owing to high binding capacity and an affinity for	Shahzad et al. (2019
MX-SA _{4:20}	116	23 334	temp. = 298 K	933	Hg^{2+} , MX-SA _{4:20} adsorbed Hg^{2+} extraordinarily	Shanzad et al. (2013
5.14.20			synthetic water	555	well even under very acidic conditions (pH $<$ 0).	
-TACSs	Pb(II)	200	pH 2-11	218	The fabrication of e-TACFs and e-TACSs was	Gu et al. (2018)
-TACFs	. ,		temp. = 298–328 K	284	performed via a hydrothermal and fluoride-free	
			synthetic water		method and the adsorption capacity for Pb(II) was	
					significantly high.	
$i_3C_2T_x$ -10%	Cr(VI)	208	pH 2-13	250	The Cr(VI) could be effectively reduced to less toxic	Ying et al. (2015)
			temp. = RT		Cr(III) species and the residual Cr(VI) in treated	
			synthetic water		water was far below the drinking water standard	
11 Tr C	6.1	10.0 500		226	recommended by the World Health Organization.	Cl. 1 . 1 . 1 . (2010
Alk-Ti ₂ C _{sheet}	Cd	19.6-562	pH 2-9	326	Ti ₂ AlC MAX phase which is exfoliated with NaOH,	Shahzad et al. (2019)
			temp. = RT		fluoride-free, could successfully adsorb both heavy	
i C T DMSO budated	11	5-220	synthetic water pH 2-6	214	metals and other contaminants. Hydrated and intercalated MXene adsorbed dye	Wang et al. (2017a)
Ti ₃ C ₂ T _x -DMSO-hydated	U	5-220	temp. = RT	214	chemicals and heavy metal ions more considerably	Wallg et al. (2017a)
			synthetic water		and their application is considered greatly	
			synthetic water		favorable.	
Γi ₃ C ₂ T _x	Cs	5-300	pH 2-12	25.4	The obtained maximum adsorption capacity of Cs ⁺	Khan et al. (2019)
3 2 A			temp. = 273–303 K		removal on Ti ₃ C ₂ T _x is due to the reaction at room	
			synthetic water		temperature within 1 min which is more effective	
					than other adsorbents.	
$Ti_3C_2T_x$	Ba	50-500	pH 1-10	12	The maximum adsorption capacity of Ba ²⁺ on Alk-	Mu et al. (2018)
Alk-Ti ₃ C ₂ T _x			temp. $= RT$	46.5	$Ti_3C_2T_x$ was 46 mg g ⁻¹ which is approximately three	
			synthetic water		times greater than unmodified $Ti_3C_2T_x$, presenting	
					important selectivity of Ba ²⁺ among other	
			*** =		inorganics.	
	Pd	100	pH 0-5	119	The interlayer structure and morphology of MXene	Mu et al. (2019)
Mxene-35 Mxene-45			temp. = 293-313 K	164	nanomaterials are greatly affected by the exfoliation	
vixene-45			synthetic water	185	temperature and the higher exfoliation temperature could yield larger d-spacing and	
					surface area.	
Γi ₃ C ₂ T _x	Cr	100	Kinetic = 14 h temp. = 298 K	80	A constant adsorption capacity (80 mg g^{-1}) can be	Tang et al. (2018)
13C21X	Ci	100	synthetic water	80	achieved by accordion-like Ti ₃ C ₂ materials when	rang et al. (2016)
			synthetic water		$m_{sorbent}/V_{solution}$ was 1 g L ⁻¹ , achieving equilibrium	
					in 8 h.	
K-HTNs	Eu(III)	20-300	pH 2-10	203	Owing to electrostatic interaction and H bonding,	Zhang et al. (2019a)
Na-HTNs			temp. = 298 K	222	Eu(III) could be exchanged with cations in the active	
			synthetic water		sites on MXene, therefore causing improved	
					sorption.	
MTC-P	Re(VII)	5-400	Kinetic = 6 h pH 1-10	42.1	The modification of Ti ₂ CT _x nanosheets produced	Wang et al. (2019)
CCNS-P			synthetic water	363	high advantage in terms of Re(VII) removal, causing	
					that the application of this technique on Tc(VII)	
					removal can have potential possibility.	
	U(VI)	5-400	Kinetic = 100 h pH 1–10	470	Over a wide pH range, the adsorbent well-adsorbed	Wang et al. (2018)
Γi ₂ CT _x			synthetic water		and decreased U(VI), reaching equilibrium within	
Γi ₂ CT _x			•		AV b and the adcorption capacity at pH 2 with	
Γi ₂ CT _x			·		48 h and the adsorption capacity at pH 3 with	
	DI (F)	40.000		140	$C_0[U(VI)]$ over 160 mg L^{-1} was 470 mg g^{-1} .	D
Γi ₂ CT _x Alk-MXene	Pb(II)	10-300	pH 1-7	140	$C_0[U(VI)]$ over 160 mg L^{-1} was 470 mg g^{-1} . The adsorbent achieved equilibrium within 2 min	Peng et al. (2014)
	Pb(II)	10-300	pH 1-7 temp. = 293-325 K synthetic water	140	$C_0[U(VI)]$ over 160 mg L^{-1} was 470 mg g^{-1} .	Peng et al. (2014)

(continued on next page)

Table 1 (continued)

MXene	Species	$C_{\rm o}$ (mg L ⁻¹)	Experimental condition	$q_{\rm m}({ m mg~g^{-1}})$	Main finding	Ref.
DL-Ti ₃ C ₂ T _x	Cu	10-350	pH 2–5.5 temp. = 298–318 K synthetic water	78.5	Owing to large surface area, functional groups and dispersibility, strong adsorption of Cu was observed and it achieved equilibrium within 3 min.	
V ₂ CT _x	U(VI)	5-120	pH 3-5 temp. = RT synthetic water	174 (q _e)	The dominant adsorption mechanism is ion-exchange and, using multilayered V_2CT_x , it achieved equilibrium after 4.5 h with different functional groups on surface. The maximum adsorption capacity (174 mg g $^{-1}$) was achieved at pH 5 when $C_0[U]$ was 100 mg L^{-1} .	Wang et al. (2016)

 C_0 = initial concentration; q_m = maximum adsorption capacity; temp. = temperature; SA = sodium alginate; TACSs = Ti₃AlC₂ nanosheets; TACFs = Ti₃AlC₂ nanosheets; DMSO = dimethyl sulfoxide; HTNs = hierarchical titanate nanostructures; PDDA = poly(diallyldimethylammonium chloride); MTC-P = multilayered Ti₂CT_x/PDDA composite; TCNS-P = Ti₂CT_x nanosheet/PDDA composite; DL = delaminated.

from the elemental compositions of used alk-MXene and XPS analysis. The elemental composition confirmed that several elements including Ti, F, Na, O, and Pb were present, and it is plausible that intercalated H⁺ or Na⁺ ions, attached to the negatively charged Ti–O, would be exchanged with Pb(II) (Giammar et al., 2007). In addition, by observing the XPS spectra, particularly the emergence of the peak of Pb and the disappeared Na 1s peak after adsorption, ion exchange could be considered the mechanism in this adsorption process (Peng et al., 2014). This is in good agreement with several other Pb adsorption studies which demonstrate that ion exchange is the adsorption mechanism of Pb (Gu et al., 2018; Zhao et al., 2011).

Besides heavy metals, radionuclides could also be adsorbed by various synthesized MXenes owing to their solid resistance against radiation (Mu et al., 2018; Wang et al., 2016, 2017a). One of the most well-known radionuclide species is uranium, and several studies have dealt with the removal of U(VI) using MXene. Experiments were conducted to investigate the removal of U(VI) by hydrated and dry Ti₃C₂T_x, which was HF-etched and intercalated with NaOH, dimethyl sulfoxide, or none (Wang et al., 2017a). The main mechanism of this U adsorption is electrostatic interaction, but considering that there was not much difference between the zeta potentials of both the original $Ti_3C_2T_x$ and intercalated $Ti_3C_2T_x$, the main influencing factor, in this case, could be the surface area and the space in between the layers. Comparing the *c* lattice parameters of the pristine Ti₃C₂T_x and the intercalated MXenes, the dry pristine MXene had the smallest *c* lattice parameter of 0.152 nm, whereas the parameters of the hydrated Ti₃C₂T_x-NaOH and Ti₃C₂T_xdimethyl sulfoxide greatly increased up to 1.228 nm and 2.018 nm. The results show that adsorption performance could greatly be influenced by intercalation and hydration of MXene. Supporting the aforementioned results, the hydrated Ti₃C₂T_x, intercalated with dimethyl sulfoxide, achieved the highest adsorption capacity of 160 mg g^{-1} , reaching equilibrium in approximately 6 h, out of all the adsorbents owing to its larger surface area, which meant it had more reactive sites on the surface. The adsorption was well explained by the Freundlich model, which can also mean that it has heterogenous adsorption sites which are the various surface functional groups in this case (Wang et al., 2017a) A separate study explored the adsorption of the radioactive Ba²⁺ ions, a homologue of ²²⁶Ra, by alk-Ti₃C₂T_x through ion exchange mechanism (Mu et al., 2018). The specific surface area of the alk-Ti₃C₂T_x, immersed in 5% NaOH, was 76.4 m² g⁻¹ whereas that of the pristine MXene was 9.78 m² g⁻¹, and this increase surface area due to immersion in NaOH enlarged the interspace of the MXene, as was also the case in other studies (Li et al., 2019; Mu et al., 2018; Peng et al., 2014; Wang et al., 2017a). After the adsorption process involving alk-Ti₃C₂T_x, it was found that the concentration of Na⁺ ions slightly increased and there was a marginal change in the concentration of H⁺ ions. This result could be because Ba²⁺ ions were captured on the alk-MXene in exchange for Na⁺ ions; the MXene has higher affinity for Ba²⁺ than H⁺ or Na⁺, thus leading to successful Ba²⁺ adsorption. The decrease of Na on the surface of alk-MXene could also be explained by the XPS results, since the peak of Na on the alk-MXene became weakened after Ba²⁺ adsorption, again owing to the ion exchange process (Mu et al., 2018). Although there are not very much studies, particularly experimental studies, on the adsorption of radionuclides and radioactive elements besides U adsorption (Zhang et al., 2016, 2017, 2018), some studies were conducted on the analogues of radionuclides, such as Eu(III) and Th(IV) (Li et al., 2019; Zhang et al., 2019a). Th(IV) adsorption on MXene was explored, and Ti₂CT_x, etched with LiF/HCl, was used as an adsorbent (Li et al., 2019). Compared to the dry adsorbent sample, much greater uptake capacity of Th (158 mg g⁻¹) was achieved by Ti₂CT_x-hydrated due to the increase in the space between layers, caused by the intercalated water molecules. The adsorption followed pseudosecond order and Freundlich model, and regarding the adsorption mechanism, Ti₂CT_x-hydrated could electrostatically adsorb positively charged Th(IV) because of its functional groups; considering the decrease of the solution pH after the adsorption process, we can conjecture that hydrogen ions were exchanged with Th(IV) by being released to water. Similar trends were often encountered in other studies regarding the sequestration of metal ions by MXenes (Mu et al., 2018; Peng et al., 2014), suggesting that the analysis is in the right track (Li et al., 2019).

MXene is intrinsically positively charged under very acidic environment and negatively charged above pH_{pzc}, which could lead to the adsorption of oppositely charged contaminants highly affected by pH. In other words, anions can be removed by positively charged MXene at very low pH, but it is hard to apply since the water quality of very low pH is not general. However, Ti₂CT_x was fabricated in order to treat ReO₄, which has some similarity with TcO₄, the ultimate target, so that related concept and insight could be obtained (Wang et al., 2019). The pristine MXene was modified with diallyldimethylammonium chloride, making the material positively charged at a wide range of pH. Both multilayered and single-layered Ti₂CT_x modified with diallyldimethylammonium chloride possessed positive charges at pH from 1 to 10, which was confirmed by their zeta potential values, compared to the nonmodified MXene with pH_{DZC} around 2 to 3. In particular, nanosheets of the modified MXene, although with a smaller surface area $(18 \text{ m}^2 \text{ g}^{-1})$ than those of the unmodified one $(31 \text{ m}^2 \text{ g}^{-1})$ because of the presumable diallyldimethylammonium chloride connecting the nanosheets, exhibited better adsorption performance over the wide range of pH from 1 to 10 than the unmodified nanosheets of the MXene, in which it could be assumed that electrostatic interaction was the dominant adsorption mechanism. Also, as an extension of adsorption, it was confirmed that some of the Re(VII) adsorbed as ReO_4^- were reduced to Re(IV), probably in the form of ReO_2 , by diallyldimethylammonium chloride (Wang et al., 2019). Reduction of inorganic ions can be found in several other studies (Wang et al., 2018; Ying et al., 2015).

3.2. Effects of water quality

3.2.1. pH

The pH value is one of the most influential factors that affect adsorption. Since the value is related to the concentration of positively charged H⁺ in water, it could affect the surface charge of MXene and the adsorptive efficiency of its surface functional groups. Under a low pH value, below pH 2 for example, abundant H⁺ ions could react, competing with positively charged ions of the target compounds, with negatively charged functional groups, such as -0, -0H, and -F, in water and eventually protonate the surface of MXene (Shahzad et al., 2017). The protonated MXene would be no longer negatively charged, which means that electrostatic attraction would not occur any longer unless the MXene is deprotonated (Gu et al., 2018). However, under high pH, there would be less concentration of H⁺, therefore MXene could remain negatively charged. This can be confirmed by measuring the zeta potential value for various pH. Generally, if the pH is below pH_{pzc} , which is the specific pH at which the zeta potential value is 0, the zeta potential value of MXene is positive, and if the pH becomes higher than pH_{pzc}, the value of the zeta potential becomes lower, which could probably be affected by functional groups on the surface of MXene (Wang et al., 2019). Higher pH value is not always preferred for heavy metal adsorption. Since, at high pH, metal ions could react with abundant amounts of hydroxide in water, although higher pH could induce more negatively charged MXene, the metal adsorption performance of MXene could be less effective at high pH (Fard et al., 2017).

One of the typical examples showing the effect of pH is the experiments on Pb²⁺ adsorption by MXene nanofiber sheets (Gu et al., 2018). At low pH, pH less than pH_{pzc} in particular, the zeta potential of MXene was positive, which means that the MXene was unlikely to adsorb Pb ions by electrostatic interaction. The results of the adsorption experiments also confirmed that below pH_{pzc} the removal percentage was low, compared to the percentage at higher pH. However, as the pH went higher than pH_{pzc}, the adsorption rate increased up to pH 7, and from pH 7 the removal rate fairly decreased, and this could be explained by the possible reaction of Pb ions and hydroxides to form metal hydroxide salts (Gu et al., 2018). These results are in good agreement with other studies on the adsorption of inorganic contaminants (Khan et al., 2019; Li et al., 2019; Mu et al., 2018; Shahzad et al., 2018; Wang et al., 2017a, 2018; Zhang et al., 2019a). Not always is the charge on MXene negative for the adsorption of inorganic contaminants in water; positively charged MXene could capture negatively charged target contaminants. In the study on Cr(VI) removal (Ying et al., 2015), since the surface charge of Ti₃C₂T_x-10% became positive when the solution pH was below pH_{pzc} , pH 2.4 in this case, the ionic form of Cr(VI), which is $Cr_2O_7^{2-}$, was attracted to the protonated functional groups of the MXene. Also, if Cr(VI) acquired enough H⁺ and electrons, it could be converted to Cr(III), and at low pH, H⁺ ions were abundant and electrons could be provided from MXene, thus offering conditions conducive for Cr(VI) to be converted to the less hazardous Cr(III) (Ying et al., 2015).

In one study, adsorption by MXene was almost independent of pH value, that is the MXene remained positively charged from pH 1 to 10. The research, on Re(VII) anion adsorption by modified MXene, was conducted, using positively charged Ti_2CT_x modified with diallyldimethylammonium chloride (Wang et al., 2019). Adsorbing anions with MXene is possible under very acidic

environment, but also a very limited option. By analyzing the zeta potential value of the modified Ti₂CT_x nanosheets, the charge on the MXene was found to be constantly positive regardless of pH value varying from 1 to 10, which was necessary to adsorb Re(VII) anions in the form of ReO₄. Subjecting the MXene to very low pH would have adversely affected its stability owing to the dissolution of Ti. However, after the modification, the extent of dissolution slightly decreased, which implies that the modification enhanced the stability of the diallyldimethylammonium chloride. In terms of their adsorption performance, the modified multilayered Ti₂CT_x achieved much less adsorption capacity with increase in the solution pH than the modified Ti₂CT_x nanosheets since the external surface area that could react with diallyldimethylammonium chloride was reduced. Therefore, the unmodified inner layers of the multilayered Ti₂CT_x could remain negatively charged, thus causing electrostatic repulsion (Wang et al., 2019).

3.2.2. Background ions and NOM

In order to examine the practicality of MXene-based adsorbent and if it is appropriate for the removal of specific target compounds in the presence of other ions and NOM which exist in municipal/industrial wastewater or effluent, the effect of background ions and NOM, such as humic acid, was investigated. For an adsorbent to be considered effective for the removal of a target compound, it must have a higher selectivity and affinity for the target material than other competing background ions (Mu et al., 2018; Wang et al., 2017a). In general, MXene-based adsorbents have high affinity for divalent cations, compared to monovalent cations, and the existence of humic acid in water may yield slightly better adsorption performance owing to a bridge effect (Jun et al., 2020b; Mu et al., 2018; Peng et al., 2014).

Since several water resources are hard, including wastewater, the effect of Ca²⁺ and Mg²⁺ on adsorption by MXene in terms of ion competition is considered worthy of attention. The affinity of alk- $Ti_3C_2T_x$ for several positively charged ions was tested: Ca^{2+} , Mg^{2+} , and the target ion, Pb²⁺ (Peng et al., 2014). The result shows that alk-MXene had higher selectivity for Pb2+ than Ca2+ or Mg2+, which is attributed to relatively low hydration energies of Pb2+ than the other cations. This was compared with the result of adsorption by ion exchange resin, and even though the initial removal rate of the resin without competing cations was higher than that of the MXene, overall uptake of Pb ions significantly decreased with increase in the concentration of Ca or Mg ions (Peng et al., 2014). Similar studies have been conducted regarding the competition of cations including Ca(II) and Mg(II), and one is a research on U(VI) removal and the possible influence of various cations (Wang et al., 2017a). The hydrated Ti₃C₂T_x-dimethyl sulfoxide showed great selectivity for U(VI) among various metal ions such as Co, Ni, Zn, Sr, La, Nd, Sm, Gd, and Yb, and the same result was also obtained in the experiment with Na⁺, Mg²⁺, and Ca²⁺, which aimed for any influence caused by ion strength (Wang et al., 2017a). Another study focusing on the competing effect of cations explored the impact of cations such as Ca²⁺, Mg²⁺, Sr, La, and Ce, which are regarded as typical ions in nuclear industry effluent, on Ba²⁺ adsorption by MXene and alk-MXene (Mu et al., 2018). It was shown that both MXene and alk-MXene achieved high removal rate of Ba²⁺, compared to their removal rates for the other cations, and in particular, alk-MXene showed almost more than 95% efficiency while MXene achieved less than 80% efficiency for Ba²⁺ adsorption, which was still higher than for the other cations. Thus, they concluded that since Ba has a smaller radius, it could be more likely for Ba ions to enter the interlayers, increasing reactive sites, and the adsorbent could have a greater affinity for the divalent ions, which is in good agreement with the findings of the previously mentioned study (Mu et al., 2018; Peng et al., 2014).

To study anion adsorption on MXene and the influence of background ions, the selectivity of diallyldimethylammonium chloride for rhenium was tested (Wang et al., 2019). Diallyldimethylammonium chloride showed a much higher selectivity for Re ions than for SO_4^{2-} and Cl^- in the presence of Re ions and other anionic ions such as SO_4^{2-} , Cl^- , ClO_4^- , and NO_3^- at pH 4, considering the distribution coefficient of more than 2.1×10^4 mL g^{-1} . However, the adsorption capacity of diallyldimethylammonium chloride for Re ion, when compared with its capacity for ClO_4^- and NO_3^- , decreased considerably due to, for ClO_4^- , its ionic radius, similar chemical formation with Re ion, and energy of hydration. In sum, NO_3^- turned out to be the most competitive and inhibiting ion, followed by ClO_4^- , Cl^- , and SO_4^{2-} , in the removal of Re ions (Wang et al., 2019).

Effects of background ions on U(VI) sequestration and reduction by Ti₂CT_x were explored using synthesized acidic wastewater from mine industries (Wang et al., 2018). In the synthesized solution, various ions, including U, Na⁺, Mg²⁺, Ca²⁺, Fe³⁺. Al³⁺, SO₄²⁻, and NH₄, were present with the MXene, and the experiments were conducted under aerobic and anaerobic conditions. A removal rate of more than 99% was achieved, while competing for other cations, under anaerobic condition for 2 d, which may be an indication that the MXene had high selectivity for U. The result regarding the U ion selectivity of MXene is in good agreement with the previous study on U capture using V₂CT_x, which exhibited great selectivity for U among other various metal cations, bolstered by the selectivity coefficient value, which was above 10 (Wang et al., 2016). However, in the presence of dissolved oxygen, the reduced U(IV), adsorbed on the MXene, was released to some extent as time passed, confirmed by the reduced removal rate below 50% after 20 d. This could be attributed to the oxidation by the dissolved oxygen of U(IV) to U(VI), which is soluble in water and whose solubility could have jeopardized both its reduction and sequestration. The effect of Fe ions, under the aforementioned conditions, on U reduction was also examined, and it turned out that the trend of release of U(VI) under aerobic condition was initially affected by Fe ions, occurring at a slightly more rapid pace than it did in the absence of Fe ions, until 13 d of reaction time had elapsed. However, after 15 d or so, the removal rate of U(VI) showed insignificant difference from the rate when Fe ions were absent, suggesting the Fe ion slightly affects U sequestration (Wang et al., 2018).

The effect of NOM on adsorption reactions involving MXene has been explored. One of the studies focused on the effect of humic acid on Pb²⁺ adsorption by MXene (Jun et al., 2020b). They conducted experiments by varying the concentration of humic acid from 0 to 10 mg L⁻¹ and examined Pb²⁺ adsorption efficiency and capacity (q_e) of Ti₃C₂T_x. According to the result, there was an increase in the efficiency and q_e value as the concentration of humic acid increased. They explained that the phenomenon might be attributed to the bridging effect of humic acid; since the behavior of humic acid resembles that of divalent anions at pH 6, humic acid might be able to bind to Pb ions, making connections like a bridge, which favored Pb²⁺ adsorption. The result is similar to the effect of divalent anions on adsorption by MXene, and the bridge effect is also mentioned in other studies (Jun et al., 2020b; Liu et al., 2018b).

3.3.3. Temperature

Temperature affects physical and chemical reactions. Increase in temperature generally leads to increased adsorption capacity. In order to evaluate the effect of temperature on adsorption, standard enthalpy, standard entropy, and standard free energy, which may be obtained by Gibbs free energy equation, can be used to verify the characteristics of the adsorption process, such as whether it is endothermic/exothermic, spontaneous/nonspontaneous, and etc. (Gu et al., 2018; Khan et al., 2019; Li et al., 2019). When temperature

rises, standard free energy decreases, but enthalpy and entropy increase. A positive value of standard enthalpy change indicates that the adsorption reaction is endothermic, a positive value of standard entropy change implies that the reaction is feasible, and a negative value of standard free energy change indicates a spontaneous reaction. According to the general trend of thermodynamic analysis, higher temperature may be beneficial to adsorption process.

The effect of temperature on adsorption reaction has been widely explored in several studies (Khan et al., 2019; Li et al., 2019; Shahzad et al., 2017, 2018). Experiments were carried out to investigate the effect of temperature on Pb adsorption by Ti₃C₂based nanomaterials etched with NaOH (Gu et al., 2018). The study showed that the adsorbent performed better at a higher temperature, demonstrated by carrying out experiments to obtain adsorption isotherms at three different temperatures: 298, 313, and 328 K. The achieved q_e value under the lowest temperature was lower than the q_e values achieved at the higher temperatures. In detail, the q_e value at 298 K was 286 mg g⁻¹, compared to the values of 380 mg g⁻¹ and 549 mg g⁻¹ achieved at 313 K and 328 K, respectively. In order to demonstrate this relationship, thermodynamic analysis was carried out by calculating thermodynamic parameters. The positive value of enthalpy change and entropy change showed that the adsorption reaction was endothermic process with high likability. Also, the negative value of free energy change showed that the reaction was spontaneous and bolstered the analysis of temperature preference by presenting lower values of free energy change as temperature increased (Gu et al., 2018). A similar study showed the temperature preference of adsorption reaction, but explained that the trend could not be related to the effect of temperature (Dong et al., 2019b). The study investigated the effect of temperature on the adsorption of Pb and Cu ions by Ti₃C₂/alginate adsorbent and observed an increasing trend of adsorption at the temperature range from 298 to 333 K. An approximately 10% increase in adsorption was observed for a 35 °C total increase in temperature. It was concluded that the increase was not significant and that the adsorbent's distinct structure could have contributed to the marginal result by ensuring that its adsorption mechanism was less dependent on temperature (Dong et al., 2019b).

A study focused on the effect of temperature on Pb adsorption by 2D MXene exhibited a behavior different from the general trend. Experiments were conducted at 293, 303, and 313 K in order to investigate the effect of temperature on MXene Pb adsorption (Mu et al., 2019). Interestingly, the values of enthalpy and entropy change were negative, unlike in other studies. For MXene-25, -35, and -45, -22.36, -22.24, and -23.10 kJ mol⁻¹ were the respective enthalpy changes and -66.34, -62.91, and -63.04 J mol⁻¹ were the respective entropy changes. Accordingly, the calculated values of the free energy change were negative, and the values of the free energy change for all the three synthesized MXenes increased approximately by 1.3 kJ mol⁻¹ on average, while the temperature increased from 295 to 313 K. In sum, all the three thermodynamic parameters turned out to be negative, which means that the adsorption reaction was spontaneous, exothermic and reversible (Mu et al., 2019).

4. Removal of organic contaminants by MXene nanomaterials

4.1. Effects of contaminant and MXene properties

Organic contaminants can also be removed from water by MXene-based adsorbents. Typical organic contaminants are dye compounds. Since MXene-based adsorbents are negatively charged in general, positively charged dye compounds, such as methylene blue, can be effectively removed from water. There are a few

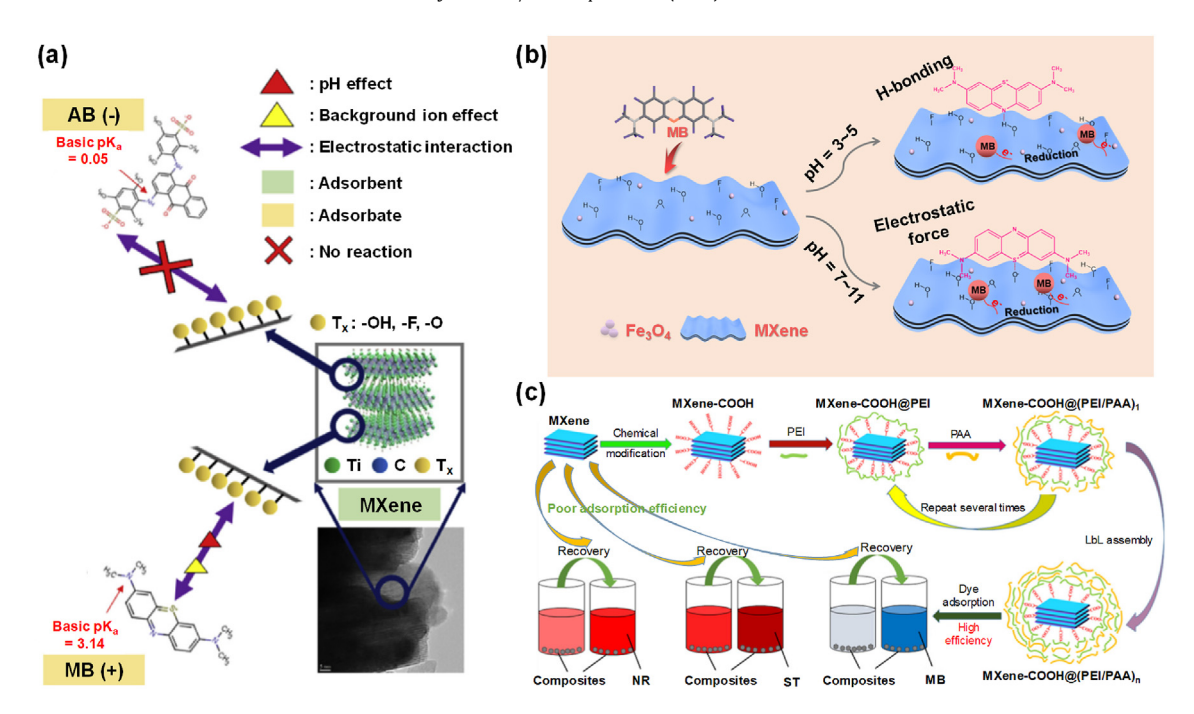


Fig. 4. (a) Plausible schematic diagram for adsorption mechanisms of methylene blue (MB) and acid blue 80 (AB) by MXene (Jun et al., 2020a). (b) Proposed mechanism for the adsorption of MB on the surface of MXene@Fe₃O₄ (Zhang et al., 2019b). (c) Schematic illustration of the fabrication of MXene-COOH and layer-by-layer -assembled composites by chemical modification and layer-by-layer self-assembly (Li et al., 2018). (For interpretation of the references to colour in this figure legend, the reader is referred to the Web version of this article.)

adsorption mechanisms, frequently mentioned in several studies on dye adsorption by MXene, which are electrostatic interaction (Huang et al., 2019; Meng et al., 2018; Rozmysłowska-Wojciechowska et al., 2019), ion exchange (Wei et al., 2018), and etc. In Fig. 4a-b, mechanisms of adsorption of dyes by MXene are illustrated. The adsorption reaction of organic contaminants, like the removal of inorganic contaminants, is highly influenced by water quality parameters such as pH, temperature, and the presence of background ions and NOM; the effect of these parameters is explained in the following section. Besides dye contaminants, more research on the removal of different organic contaminants, such as urea (Meng et al., 2018), lysozyme (Rozmysłowska-Wojciechowska et al., 2019) and deoxyribonucleic acid (Huang et al., 2019), has been explored for various potential applications. In addition, the removal of organic contaminants by gaseous adsorption on MXene has been investigated for the adsorption of air pollutants such as aroma molecules (Ciou et al., 2019), carbon dioxide (Morales-García et al., 2018), and methane (Liu et al., 2016, 2017a). Table 2 presents the adsorptive removal of selected organic contaminants by MXene nanomaterials.

Dye adsorption on MXene was exhibited, which used methylene blue and acid blue 80 as adsorbates and ${\rm Ti}_3{\rm C}_2{\rm T}_{\rm X}$ as the adsorbent (Mashtalir et al., 2014). The dyes, methylene blue and acid blue 80, were representative of cationic and anionic dye, respectively. From the analysis of the adsorption isotherm it was found that the adsorption of methylene blue followed the Freundlich isotherm model more than Langmuir isotherm model, and this conclusion was arrived at after comparing the Pearson's correlation coefficients of both isotherm models. Following the Freundlich model may imply that the adsorbent had heterogenous adsorption sites, and this is supported by the fact that various functional groups, such as -F, -OH, and -O, of the MXene took part in the adsorption reaction. The adsorption capacity of methylene blue was up to 39 mg g $^{-1}$, which is smaller than the that of commercially available activated carbon but comparable to those of adsorbents with

similar surface areas or structures. On the other hand, acid blue 80 was not adsorbed on the MXene since the dye is negatively charged, like the adsorbent, causing electrostatic repulsion. After 2 h of adsorption of methylene blue, the adsorption reaction weakened over time, and this may be attributed to the oxidation of MXene and change in the structure of the adsorbent owing to the intercalation of the adsorbate molecules, which resulted in flawed stacking (Mashtalir et al., 2014).

The effect of intercalation on methylene blue adsorption was explored with three adsorbent (MXenes) kinds: Ti₃C₂T_x-hydrated, Ti₃C₂T_x-dimethyl sulfoxide-hydrated, and Ti₃C₂T_x-dry (Wang et al., 2017a). Comparing the adsorption capacity of the adsorbents, it was observed that Ti₃C₂T_x-dimethyl sulfoxide-hydrated achieved an uptake capacity of 125 mg g⁻¹, showing 99.8% removal of methylene blue, which was much higher than the 78 mg g^{-1} achieved by $Ti_3C_2T_x$ -hydrated and the 8 mg g⁻¹ by $Ti_3C_2T_x$ -dry. The enlarged space between layers brought about by the effect of the intercalation with dimethyl sulfoxide resulted in the availability of more adsorption sites for the methylene blue molecules. The intercalation of dimethyl sulfoxide could also have led to the cointercalation of methylene blue, thus expanding the space between layers even more. Water molecules might have played the role of intercalant for Ti₃C₂T_x-hydrated, leading to a reasonable adsorption performance much greater than that of Ti₃C₂T_x-dry (Mashtalir et al., 2014). Intercalation using the alkaline solutions, LiOH, NaOH, and KOH, was also found to affect methylene blue adsorption on Ti₃C₂T_x (Wei et al., 2018). Based on the ionic radius of Li, Na, and K, the ion having a smaller radius, such as Li⁺ and Na⁺, could be loaded more than the one having a larger radius, K⁺ in this case; Na ions and Li ions were likely to be piled twice or thrice while K ions might hardly stack once. This resulted in the difference in the enlarged spaces in between the layers of the MXenes for the adsorbents treated with KOH, NaOH and LiOH, confirmed by their respective c lattice parameters of 2.49, 2.62, and 2.64 nm. On the other hand, the adsorption performance of the three MXenes did

 Table 2

 Summary of adsorptive removal of selected organic contaminants by MXene nanomaterials.

MXene	Species	$C_{\rm o}$ (mg $\rm L^{-1}$)	Experimental condition	$q_{ m m}$ (mg g $^{-1}$)	Main finding	Ref.
$Ti_3C_2T_x$	Methylene blue	50	Kinetic = 8 h temp. = 293 K synthetic water	38.9	The adsorption of methylene blue on $Ti_3C_2T_x$ was not extremely effective, compared to activated carbon, but, considering its unique properties and possible application, $Ti_3C_2T_x$ could be decent adsorbent.	Mashtalir et al. (2014)
$Ti_3C_2T_x$ $LiOH-Ti_3C_2T_x$ $NaOH-Ti_3C_2T_x$ $KOH-Ti_3C_2T_x$	Methylene blue	50	Kinetic = 3 h temp. = 298 K synthetic water	99.9 121 189 77	The alkali-treated adsorbent has enhanced interlayer spacing and surface functional group, resulting in improved adsorption performance.	Wei et al. (2018)
Ti ₃ C ₂ T _x	Urea	30–450 mg/ dL	Kinetic = 1 h temp. = RT-333 K synthetic water/Dialysate	21.7	The q_m (21.7 mg g^{-1}) was calculated by Langmuir-Freundlich model at 310 K. The finding exhibited rapid and selective adsorption of urea on MXene and the adsorption capacity reached 94%, showing no important impact on cell viability and hemocompatibility.	Meng et al. (2018)
$Ti_3C_2T_x$	Methylene blue	5-40	pH 3.5–9.5 temp. = 293–313 K synthetic water	140	MXene achieved equilibrium in a short amount of time (within 30 min) and the main mechanism of the adsorption was electrostatic interaction between MXene and Methylene blue.	
Ti ₃ C ₂ T _x -dry Ti ₃ C ₂ T _x -hydrated Ti ₃ C ₂ T _x -DMSO-hydrated	Methylene blue	100	Kinetic = 6 h temp. = RT synthetic water	8 78 125	Important MB adsorption capacity was exhibited in the adsorption result of $Ti_3C_2T_{x^-}$ DMSO-hydrated, up to 125 mg g ⁻¹ , compared to other adsorbents.	Wang et al. (2017a)
MXene MXene-COOH MXene-COOH@(PEI/ PAA) ₁₀	Methylene blue	10	Kinetic = 200 min temp. = 298 K synthetic water	86.8 71 82	The MXene-COOH@(PEI/PAA) _n was employed to determine the adsorption capability of three different dyes and the target contaminants were effectively adsorbed owing to its layered structure and modified functional groups.	
MXene@Fe ₃ O ₄	Methylene blue	1-40	pH 3-11 temp. = 298-328 K synthetic water	11.7	The key mechanism in the pH above 5.1 is electrostatic force due to pH _{pzc} of the adsorbent. In addition, other adsorption mechanism could be owing to the Ti site and OH groups.	
Ti ₃ C ₂ —SO ₃ H	Methylene blue	25–250	pH 2-12 temp. = 318–358 K synthetic water	723	The maximum adsorption capacity at $C_0[MB] = 250 \text{ mg L}^{-1}$, 298 K and pH 7 was 723 mg g ⁻¹ . By exhibiting the different adsorption capacity between pristine Ti_3C_2 (21 mg g ⁻¹) and Ti_3C_2 – SO_3H (111 mg g ⁻¹), it proved that Ti_3C_2 – SO_3H can be an ideal adsorbent.	Lei et al. (2019)

 $C_0=$ initial concentration; $q_m=$ maximum adsorption capacity; temp. = temperature; PEI = polyethylene polyimide; PAA = poly acrylic acid.

not follow the increasing order of the expanded spaces, as confirmed by the isotherm experiment; NaOH–Ti₃C₂T_x achieved the highest adsorption capacity of 189 mg g⁻¹, followed by LiOH–Ti₃C₂T_x (121 mg g⁻¹), pristine Ti₃C₂T_x (100 mg g⁻¹), and KOH–Ti₃C₂T_x (77 mg g⁻¹). The result of the LiOH-treated MXene indicates that the expansion of the interlayer spaces led to the exfoliation of the layers, thus causing the MXene to experience no effect due to the intercalation of the cations and, accordingly, decreasing the adsorption capacity more than expected. It was concluded, for KOH–Ti₃C₂T_x, that the enlarged space might inhibit complete activation of the adsorbent (Wei et al., 2018).

The adsorption of three kinds of dye compounds by MXene-based nanocomposites modified by layer-by-layer strategy was investigated (Li et al., 2018). Pristine MXene was first treated with chloroacetic acid to obtain a COOH-modified surface, and then immersed in polyethylene polyimide and poly acrylic acid solutions separately for multiple times in order to have several layers of polyethylene polyimide and poly acrylic acid molecules obtaining 3-dimensional formation. The schematic illustration of the fabrication process is shown in Fig. 4c. The fabricated material, MXene-COOH@(polyethylene polyimide/poly acrylic acid)₁₀, was utilized, as well as the pristine MXene and MXene-COOH, to examine and compare the adsorption of methylene blue, safranin *t*, and neutral red. The result showed that MXene-COOH@(polyethylene

polyimide/poly acrylic acid) $_{10}$ achieved the highest adsorption capacity among the three prepared adsorbents, followed by MXene-COOH, and then the pristine material. The result followed the pseudo-second-order kinetic model and showed that the reaction was affected by increase in temperature, confirmed by the results obtained for conducting the adsorption experiments at temperatures of 298, 308, and 318 K. From the analysis of the adsorption isotherm model it was found that the pristine MXene and MXene-COOH followed the Freundlich isotherm model, as confirmed by the R^2 value. However, MXene-COOH@(polyethylene polyimide/poly acrylic acid) $_{10}$ followed the Langmuir isotherm model, indicating that the reaction was a monolayer adsorption and the adsorbent had homogeneous adsorption sites (Li et al., 2018).

4.2. Effects of water quality

4.2.1. pH

The pH greatly affects the performance of MXene-based adsorbent in regard to the removal of organic compound. Basically, since the dominant mechanism of adsorption is electrostatic interaction, regardless of whether the contaminant is an organic or inorganic compound, the charges on the adsorbent and adsorbate are very important (Jun et al., 2020a; Lei et al., 2019). The pK_a value of the adsorbate and the pH_{pzc} of the adsorbent can affect the adsorption

process, depending on the solution pH, and considering the general trend, adsorption performance is enhanced as pH value increases. Under acidic conditions, MXene cannot be negatively charged enough to attract positively charged adsorbates, since there is competition for the MXene ions between the H⁺ and adsorbate ions, such as methylene blue. Under alkaline conditions, owing to the sufficient negative charge of the adsorbent, more adsorption can be expected (Jun et al., 2020a; Lei et al., 2019).

The effect of solution pH on adsorption by MXene was examined using Ti₃C₂T_x as an adsorbent and methylene blue as an adsorbate (Jun et al., 2020a). The experiments were conducted at solution pH of 3.5, 7, and 9.5, and it was observed that as the solution pH increased, the adsorption capacity and removal rate increased. This demonstrates that the dominant mechanism was electrostatic interaction, affected by pK_a value of methylene blue and pH_{pzc} of Ti₃C₂T_x. Since methylene blue is positively charged at pH 3.1 and has Cl⁻, it can be attracted by a negatively charged adsorbent at the same pH. And the pH_{pzc} of the MXene was approximately pH 3, which led to the adsorption of methylene blue on the adsorbent in this study (Jun et al., 2020a). The effect of pH on adsorption was also investigated, and the study employed Ti₃C₂-SO₃H as an adsorbent and methylene blue as an adsorbate in water (Lei et al., 2019). The investigation was conducted at pH 2 to 12, and the lowest adsorption capacity of 49 mg g⁻¹ was achieved at pH 2 and the highest capacity of 145 mg g^{-1} at pH 11. This relationship between adsorption capacity and pH could be explained by the adsorption mechanism applied in this reaction, which is electrostatic interaction. At low pH, in the abundance of H ions, there would be competition for the adsorbent ions between the hydrogen ions and adsorbate ions, leading to less adsorption capacity. On the other hand, at high pH, the MXene-based adsorbent would be more negatively charged due to more SO₃ on the surface, leading to its higher attraction for the positively charged methylene blue in water

An interesting study on the pH effect of methylene blue adsorption by MXene was carried out (Zhang et al., 2019b). pH value was varied from pH 3 to 11 and the adsorption capacity at each pH level was noted. Around 10 mg g^{-1} of adsorption capacity was achieved at pH 3 and 11, unlike in other studies. The adsorption capacity decreased from pH 3 until pH 7 and increased from pH 7 to 11; that is to say, the minimum adsorption capacity of around 2 mg g⁻¹ was obtained at pH 7. Since high adsorption capacity was obtained below the pH_{pzc} , which was pH 5.1 in this study, it is likely that the main adsorption mechanism at pH 3 was not electrostatic interaction but hydrogen bonding. And the increasing trend of the adsorption capacity from pH 7 may imply that the negatively charged MXene, confirmed by the zeta potential analysis, attracted the positively charged adsorbate. However, due to the possibility of hydrolysis of methylene blue at high pH, adsorption performance at high pH was slightly lower than at low pH (Zhang et al., 2019b).

4.2.2. Background ions and NOM

There is need to examine the interaction of adsorbate, adsorbent, and pre-existing ions in water for practical application. This is because, in untreated water, including municipal and industrial wastewater, adsorption might be inhibited by pre-existing ions and NOM, a typical example being humic acid (Jun et al., 2020b). As a result, several studies have explored the effect of background ions, related to ion strength, and NOM on adsorption reaction (Lian et al., 2015; Xu et al., 2008). The effect of background ions may vary depending on their charges, and it has been found that the presence of pre-existing ions can enhance or worsen the performance of adsorbents (Jun et al., 2020a).

In order to investigate the effect of background ions, adsorption experiments in the presence of background ions, such as those from NaCl, CaCl₂, and Na₂SO₄, were conducted, and in the experiments the concentrations of the reagents were varied (Jun et al., 2020a). The reagents were selected such that the different effects between monovalent ions and divalent ions, if any, would be highlighted. As the concentration of NaCl increased from 300 to 1200 μS cm⁻¹, the adsorption capacity of MXene and its removal rate of methylene blue decreased, and this phenomenon might be attributed to screening effect, which reduced the electrostatic attraction between the adsorbate and MXene. The divalent ions of CaCl2 and Na₂SO₄ in this study showed a slightly different trend of result, depending on how the ions and adsorbate were charged. Due to the effect of the divalent cations, Ca²⁺ in this case, which was as a result of the competition for MXene between the cations and methylene blue, a decrease in the adsorption capacity and removal rate was observed. On the other hand, the divalent anions, which are oppositely charged to the adsorbate, rarely affected the adsorption (Jun et al., 2020a).

The effect of NOM was also evaluated in the same study; the effect of humic acid on adsorption was explored (Jun et al., 2020a). Experiments were conducted in the presence of humic acid at concentrations of 0, 2.5, and 10 mg L⁻¹, and changes in the adsorption capacity and removal rate due to the varying concentrations of humic acid were observed. As the concentration of humic acid increased, the adsorption capacity of MXene and the rate of removal of methylene blue increased. The result may be explained with the aid of the bridge effect, as mentioned in Section 3.2.2., where the effect of humic acid on the adsorption of inorganic contaminants has been treated (Jun et al., 2020b; Liu et al., 2018b). Since humic acid has aromatic structure and carboxylic acid, which makes it likely to act as a multivalent anion, the effect of humic acid on adsorption could be similar to the effect of background ions, divalent anions in particular (Jun et al., 2020a).

4.2.3. Temperature

The effect of temperature on adsorption in water by MXene, like other factors, has been investigated and found to be substantial. When temperature increases, the viscosity of water generally decreases, leading to greater diffusion in the system and, thus, increased possibility for adsorption (Lei et al., 2019; Zhu et al., 2019). Also, temperature can influence thermodynamic parameters, including enthalpy, entropy, and Gibbs free energy. Increased temperature results in a positive value of enthalpy change before and after reaction, which indicates that the reaction is endothermic. Furthermore, by evaluating values of entropy change and Gibbs free energy change, it can be predicted if the reaction would be spontaneous or not (Jun et al., 2020a; Lei et al., 2019; Zhang et al., 2019b; Zhu et al., 2019).

The effect of temperature on the adsorption of contaminants in water was evaluated, using ${\rm Ti}_3{\rm C}_2{\rm T}_{\rm X}$ for the removal of methylene blue at the specific temperatures 293, 303, and 313 K (Jun et al., 2020a). Analyzing for the adsorption capacity, it was found that the adsorption process was enhanced and removal rate increased as temperature increased. This relationship was demonstrated by the thermodynamic parameters: positive values of enthalpy and entropy changes and negative value of Gibbs free energy change. The positive value of enthalpy showed that the reaction was endothermic, and the positive value of entropy change referred to the increased randomness. As the temperature increased from 293 to 313 K, Gibbs free energy decreased — -8.99 kJ mol $^{-1}$ at 293 K, -9.79 kJ mol $^{-1}$ at 303 K, and -10.51 kJ mol $^{-1}$ at 313 K - showing that higher temperature yielded better adsorption performance (Jun et al., 2020a).

The effect of temperature on methylene blue adsorption by Ti_3C_2 – SO_3H was investigated (Lei et al., 2019), who conducted experiments at various temperatures, from 320 to 360 K. The

adsorption capacity was first analyzed and it was concluded that higher temperatures yielded greater adsorption capacity; there was a 16 mg g $^{-1}$ increase in q_e when temperature increased from 318 to 358 K. Owing to the increased mobility due to increase in temperature, diffusion was increased, enhancing the adsorption process. On the thermodynamic parameters: the positive value of enthalpy indicates that the reaction was endothermic; the negative value of Gibbs free energy change indicates that the reaction was spontaneous, and as the temperature increased, the value of Gibbs free energy change became more negative, showing the positive influence of temperature on the adsorption process (Lei et al., 2019).

Adsorption experiments were conducted using 2D-MX@Fe₃O₄ as an adsorbent and methylene blue as an adsorbate at specific temperatures: 298, 313, and 328 K (Zhu et al., 2019). According to the adsorption result, maximum adsorption capacity (q_m) increased as temperature increased, achieving almost 92% removal of methylene blue at 328 K. The possible reasons for the increased adsorption capacity due to increased temperature were explained: such as the weak binding force at increased temperature, reduced viscosity of the solution, and expanded free volume of the system. Thermodynamic analysis was also explored, and it turned out that positive values of enthalpy, entropy and Gibb's free energy change were obtained. In particular, the value of enthalpy change, 42.8 kJ mol⁻¹, was considered high, over 40 kJ mol⁻¹, which also means that chemical interactions were involved in the adsorption process between the adsorbent and methylene blue (Zhou et al., 2017). As temperature increased, the change in free energy decreased, reaching almost 0 kJ mol⁻¹ at 328 K, and considering the positive values of entropy and free energy change, this demonstrates that the spontaneity of the adsorption reaction was affected by temperature (Zhu et al., 2019). A similar study demonstrated the importance of the effect of temperature to the adsorption performance of MXene@Fe₃O₄ (Zhang et al., 2019b). In the study, experiments at temperatures of 298, 308, 318, and 328 K were conducted. The adsorption reactions at high temperatures yielded higher adsorption capacities; in other words, the adsorption process was endothermic. Furthermore, thermodynamic analysis was carried out by examining the three parameters — entropy change, enthalpy change and Gibbs free energy change. A positive value of enthalpy change was obtained, indicating that the reaction was endothermic, a result which corroborated the results obtained from the analysis of the adsorption capacity. As temperature increased, Gibbs free energy decreased, demonstrating that higher temperature resulted in better reaction performance. The positive values of the entropy and Gibbs free energy implies that the adsorption reaction was spontaneous, although this depends also on the reaction temperature (Zhang et al., 2019b).

5. Regeneration of MXene nanomaterials

Recyclability of an adsorbent is a key factor to be considered when determining its effectiveness and economical advantage (Khan et al., 2019). Several studies have explored the regeneration of MXene-based adsorbents, showing their high reusability. The regenerants commonly used in these studies are HCl (Dong et al., 2019a; Fard et al., 2017; Khan et al., 2019; Shahzad et al., 2018, 2019a), HNO₃ and/or Ca(NO₃)₂ (Dong et al., 2019b; Peng et al., 2014; Shahzad et al., 2017; Wang et al., 2017a), and other regenerants, such as ethanol (Li et al., 2018; Zhang et al., 2019b), NaOH (Zou et al., 2016), and thiourea (Mu et al., 2019), were also used. Table 3 presents the summary of regeneration methods of exhausted MXene-based adsorbents. The recyclability of used Ti₃C₂T_x for the removal of Cs ions was examined using 0.2 M of HCl to desorb the ions (Khan et al., 2019). By adding HCl solution, the

concentration of H ions increased and there was competition between the adsorbed target contaminant and H ion for accessible surface sites on the Ti₃C₂T_x, causing the desorption of the contaminant from the MXene. Also, under highly acidic environment, desorption of the adsorbate may be accelerated since MXene tends to become positively charged due to protonation. In this study, the removal rate of the adsorbent remained over 90% after 5 regenerations and its morphology was hardly changed. However, there was a slight decrease in the removal rate with more regenerations, which may be attributed to the decrease in the number of functional groups on the surface of the adsorbent (Khan et al., 2019). The effect of the concentration of regenerant was investigated using different concentrations of HCl solution: 2, 4, 5, and 8 M (Shahzad et al., 2019a). They conducted experiments to investigate the reusability of MX-SA_{4:20}, which had been used in the adsorptive removal of Hg(II), and almost 80% of desorption of the Hg(II) ions was achieved by 2 M of HCl. Furthermore, as the concentration of HCl solution increased, the desorption rate of Hg^{2+} increased, until approximately 100% of desorption was achieved by 8 M of HCl (Shahzad et al., 2019a). A previous study on the recyclability of MXene-based nanocomposites had been conducted as part of the study on the removal of Hg(II) (Shahzad et al., 2018). They also used 1 M of HCl solution as regenerant for the exhausted MGMX in order to desorb the adsorbed mercury ions. The achieved desorption rate was approximately 90%, showing fairly constant values, but the removal rate of the adsorbent decreased from almost 100%-81.0% after five recycles. This decrease may be explained by the loss of surface functional groups and the decreased specific surface area caused by partial oxidation of the adsorbent to TiO₂ (Shahzad et al.,

Another widely used regenerant is HNO₃ or/and Ca(NO₃)₂, and being an acidic solution, similar effects as HCl solution can be achieved. A study on the regeneration of used MXene by HNO₃ or/ and Ca(NO₃)₂ was conducted, in which exhausted DL-Ti₃C₂T_x was regenerated by HNO₃ and Ca(NO₃)₂ (Shahzad et al., 2017). The adsorbent was used to remove Cu(II) in water and recycled by the acidic solution of nitric acid and calcium nitrate. The adsorption rate of the adsorbent after the first regeneration cycle was 80%, and a declining trend in the adsorption rate after the second and third cycles was observed, reaching 47 and 30%, respectively, which are steep decrease compared to the results of similar studies. The decrease might be due to imperfect desorption of copper ions, oxidation of the adsorbent, and reduction of Cu(II) to Cu(I) (Shahzad et al., 2017). Nitric acid alone may be a good regenerant, and recycle experiments of synthesized adsorbents were conducted to compare the crosslinked MXene/alginate composite, prepared with calcium nitrate, and the un-crosslinked one (Dong et al., 2019b). A 0.1 M of nitric acid was used and the regenerations of the adsorbents after the removal of Pb(II) and Cu(II) were conducted on 10 occasions in order to achieve the adsorption rate for each cycle. Since the structure of the crosslinked MXene/ alginate composite was mechanically more beneficial than the uncrosslinked composite, the adsorption rates of the former for each of the 10 cycles were higher than the ones of the latter. By increasing the stability of the structure by crosslinking with calcium nitrate, a higher adsorption rate was achieved compared to the un-crosslinked composite (Dong et al., 2019b).

6. Conclusions and areas of future study

In the various studies covered in this review paper, there are two mechanisms of adsorption for the removal of both inorganic and organic compounds which are mentioned the most: electrostatic interaction and ion exchange. Large surface areas and an abundance of surface functional groups can lead to higher adsorption,

Table 3Summary of regeneration methods of exhausted MXene-based adsorbents.

MXene	Species	Regenerant	Experimental condition	Main finding	Ref.
Ti ₃ C ₂ T _x	Ва	69% HCl	pH < 3	Regeneration of MXene could be influenced by pH since importantly less adsorption occurred in the pH below pH _{pzc} of MXene owing to the accordingly increased zeta potential value.	Fard et al. (2017)
MX-SA _{4:20}	Hg	2, 4, 6 and 8 M HCl	Contact time = 5 h (agitation)	The regeneration using 8 M HCl achieved 99% of desorption of Hg ²⁺ adsorbed on the sample, therefore causing that desorption of Hg ²⁺ from MX-SA _{4:20} , should be performed under very high acidic condition for improved result.	Shahzad et al. (2019a)
DL-Ti ₃ C ₂ T _x	Cu	HNO ₃ , Ca(NO ₃) ₂	$Contact \ time = 5 \ h$	The adsorption efficiency of regenerated DL- $Ti_3C_2T_x$ was 80% in the first cycle, 47% and 30% in the second and third cycle which could be owing to imperfect desorption of Cu^{2+} and the partial oxidation changing $Ti_3C_2T_x$ into TiO_2 .	
MGMX	Hg	1 M HCl	$Contact\ time = 5\ h\ (incubator\ shaker)$	The adsorption efficiencies of recycled MGMX were important which were higher than 90% until the fourth cycle and there was a slight decrease in the fifth cycle: 81%, attributed to the stability of MGMX.	Shahzad et al. (2018)
Glu@TNFs-3	Cd(II)	0.2 M HCI	Contact time = 9 h (stirring)	By the adsorption capacity of the recycled Glu@TNFs-3 which was 61 mg ${\rm g}^{-1}$, high reusability of the adsorbent was exhibited. Under acidic condition, the used adsorbent was protonated by ${\rm H}^+$, causing the adsorbed heavy metals to be desorbed.	
MXene-COOH@(PEI/ PAA) ₁₀	Methylene blue	C ₂ H ₅ OH	Temp. = RT	The removal rate was 85% after the first cycle and constantly decreased to 64% in the eighth cycle. The possible reasons for the decrease could be due to multiple surface washing and the loss of surface functional groups.	Li et al. (2018)
Alk-MXene	Pb(II)	0.1% HNO ₃ + 5% Ca(NO ₃) ₂		By using the regenerant HNO ₃ and Ca(NO ₃) ₂ , the used adsorbent could be efficiently recycled and the removal of Pb(II) after regeneration was 95%.	-
urchin-like rutile TiO ₂ —C	Cr(VI)	5% NaOH	Temp. = 298 K	After regeneration of u-RTC using NaOH solution, the adsorbed Cr(VI) was well desorbed and the according adsorption efficiencies of Cr(VI) were over 90% until fifth cycle.	Zou et al. (2016)
Ti ₃ C ₂ T _x -DMSO- hydrated	U(VI)	0.01, 0.1 and 0.2 M HNO ₃	$Contact \ time = 0.5 \ h$	The regeneration experiments were conducted with different concentration of the regenerant. The desorption efficiency of 0.01 M HNO ₃ was approximately 86% which is the smallest rate among the results. By increasing the concentration of the regenerant, the efficiency also increased, specifically 96% for 0.1 M and 98% for 0.2 M.	Wang et al. (2017a)
Ti ₃ C ₂ T _x	Cs	0.2 M HCI	Contact time = 0.5 h (rocking mixer) m/V = 5 g L^{-1} temp. = 293 K	The removal efficiency after the first regeneration cycle was 98% and the percentage decreased until the fifth cycle down to 91%. The possibility of the decrease could be loss of functional groups on surface and the integrity of the adsorbent.	
$Ti_3C_2T_x$	Methylene blue	0.1 N HCl, 0.1 N NaOH	$\begin{aligned} & \text{Contact time}_{HCI} = 4 \text{ h} \\ & \text{Contact time}_{NaOH} = 4 \text{ h} \end{aligned}$	The regeneration tests were conducted 4 times and there was a slight decrease in the removal rate of MB, probably due to incomplete desorption. However, the fourth regenerated adsorbent still had a q_e over $50~{\rm mg~g^{-1}}$.	Jun et al. (2020a)
MXene-45	Pd	0.5 M HNO ₃ , 0.5 M HCl, 0.5 M Thiourea (CH ₄ N ₂ S), 0.5 M HCl + 0.5 M Thiourea		Among the regenerants, 0.5 M Thiourea was the most efficient eluent with the efficiency of 99%. And, also, using 0.5 M Thiourea, the adsorption capacity was decreased from 185 mg g ⁻¹ to 167 mg g ⁻¹ but, still, the removal efficiencies were approximately over 90% until the fifth cycle.	Mu et al. (2019)
MXene@Fe₃O₄	Methylene blue			The exhausted adsorbent was washed thoroughly with ethanol and dried at 343 K. The removal efficiency was over 80% in the first cycle and there was a slightly decreasing trend of the removal efficiency down to 77% in the fifth cycle.	
Sodium alginate/ Ti ₃ C ₂ T _x	Pb Cu	0.1 M nitric acid solution		The regeneration result was different compared to cross-linked processing and uncross-linked processing. Since the cross-linking improves the mechanical properties of alginate, it showed better adsorption efficiency compared to the other.	Dong et al. (2019b)

 $MGMX = magnetic Ti_3C_2T_x MXene; TNFs = Ti_3AlC_2-derived nanofibers.$

and the adsorptive performance of MXene-based materials can be highly influenced by water quality. The main determinants of water quality that influence the adsorption performance of MXene are pH value, temperature, and background ions/NOM. Under acidic conditions, adsorption capacity, in general, decreases due to competition for MXene ions between abundant hydrogen ions and target compounds. On the other hand, as pH value increases, adsorption capacity also increases since surface charges become more negative, confirmed by the zeta potential value. At very high pH, however, decrease in adsorption capacity is observed, since abundant OH⁻ reacts with the target compound to form a hydroxide. However, there are still several studies in which the results were contrary to the general trend above, such as exhibiting adsorption almost independently of pH value. Higher temperatures generally enhance adsorption, and MXenes show higher adsorption capacity in such conditions. Confirmed by the thermodynamic parameters, the adsorption process tends to be endothermic and spontaneous, thus raising the feasibility of the adsorption reaction in regard to the increased temperature. The effect of background ions and NOM was also covered in the studies, and the presence of background ions and NOM affect the selectivity of MXene-based adsorbents for target compounds. Various ions, which are expected to exist in wastewater from a particular industry containing a target contaminant, were tested to confirm that MXene-based adsorbents could attack their target contaminants in the presence of background ions in the same solution. Most of the studies found that the adsorbents exhibited selectivity for their target contaminants and, even when they tended to adsorb the background ions, they showed greater affinity for divalent and multivalent ions than for monovalent ions, and this is similar to the behavior in the presence of humic acid. The recyclability of adsorbents is becoming important in a bid to boost their cost-effectiveness. Regeneration experiments were conducted using various cleaning agents, such as HCl, HNO₃, NaOH, C₂H₅OH, and etc. Adsorbate removal rates of MXenebased adsorbents after several regenerations were noted, and although the removal rates in most studies showed slight decrease, they still remained high, around 80–90%, showing great reusability and practicality of the adsorbents in terms of cost.

MXene has desirable features meant for successful adsorptive performance. A unique structure, which makes it possible for it to achieve larger interspaces, an enlarged surface area, and more reactive sites and functional groups on its surface are the dominant strength of MXene, leading to its high removal rate of target contaminants. However, several other areas should be further explored in order to better assess the effectiveness and practicality of MXene. While this study convers the effects of various water quality conditions including pH, background ions, NOM, and temperature, additional water chemistry conditions such as salinity, turgidity, alkalinity, and oxidants/reductants still need to be considered as well. Another area is the stability of MXene in the long run. Although MXene showed great recovery after several cycles of regeneration in most of the studies, some defect was observed in its structure, causing slightly less effective performance. And, after being stored in water for a long period of time, it was observed that the structure of MXene changed due to the formation of titanium dioxide. Hence, the stability of MXene in the long run should be studied in order to improve the cost-effectiveness, which is essential for every good adsorbent. Another area for future studies is the effect of NOM, such as humic acid and fulvic acid. The effect of NOM on adsorption by MXene is covered in this paper, but still more studies on this subject are needed since there are not much research on the effect of NOM with respect to the behavior of the acids during adsorption processes utilizing MXene-based adsorbent. With regard to the toxicity of MXene, the potential impact of the adsorbent on the health of living organisms should be thoroughly investigated before application. If found efficient in the aforementioned areas, MXene would prove its practicality as a powerful adsorbent even more and could be employed in various fields as well, not only in water treatment.

Declaration of competing interest

The authors declare that they have no known competing financial interests or personal relationships that could have appeared to influence the work reported in this paper.

Acknowledgements

This research was funded by the Korea Ministry of Environment (The SEM projects; 2018002470005, South Korea) and the U.S. National Science Foundation (OIA-1632824). This study was also supported by the University of South Carolina ASPIRE program.

References

- Al-Hamadani, Y.A.J., Jun, B.-M., Yoon, M., Taheri-Qazvini, N., Snyder, S.A., Jang, M., Heo, J., Yoon, Y., 2020. Applications of MXene-based membranes in water purification: a review. Chemosphere 254, 126821.
- Alhabeb, M., Maleski, K., Anasori, B., Lelyukh, P., Clark, L., Sin, S., Gogotsi, Y., 2017. Guidelines for synthesis and processing of two-dimensional titanium carbide (Ti₃C₂T_x MXene). Chem. Mater. 29 (18), 7633–7644.
- Anasori, B., Lukatskaya, M.R., Gogotsi, Y., 2017. 2D metal carbides and nitrides (MXenes) for energy storage. Nat. Rev. Mater. 2 (2), 1–17.
- Atkovska, K., Lisichkov, K., Ruseska, G., Dimitrov, A.T., Grozdanov, A., 2018. Removal of heavy metal ions from wastewater using conventional and nanosorbents: a review. J. Chem. Technol. Metall. 53 (2), 202–217.
- Backes, C., Higgins, T.M., Kelly, A., Boland, C., Harvey, A., Hanlon, D., Coleman, J.N., 2017. Guidelines for exfoliation, characterization and processing of layered materials produced by liquid exfoliation. Chem. Mater. 29 (1), 243–255.
- Berrios, M., Martín, M.Á., Martín, A., 2012. Treatment of pollutants in wastewater: adsorption of methylene blue onto olive-based activated carbon. J. Ind. Eng. Chem. 18 (2), 780–784.
- Blöcher, C., Dorda, J., Mavrov, V., Chmiel, H., Lazaridis, N.K., Matis, K.A., 2003. Hybrid flotation—membrane filtration process for the removal of heavy metal ions from wastewater. Water Res. 37 (16), 4018–4026.
- Burakov, A.E., Galunin, E.V., Burakova, I.V., Kucherova, A.E., Agarwal, S., Tkachev, A.G., Gupta, V.K., 2018. Adsorption of heavy metals on conventional and nanostructured materials for wastewater treatment purposes: a review. Ecotoxicol. Environ. Saf. 148, 702—712.
- Chang, F., Li, C., Yang, J., Tang, H., Xue, M., 2013. Synthesis of a new graphene-like transition metal carbide by de-intercalating Ti₃AlC₂. Mater. Lett. 109, 295–298.
- Ciou, J.H., Li, S., Lee, P.S., 2019. Ti₃C₂ MXene paper for the effective adsorption and controllable release of aroma molecules. Small 15 (38), e1903281.
- Dabrowski, A., Hubicki, Z., Podkoscielny, P., Robens, E., 2004. Selective removal of the heavy metal ions from waters and industrial wastewaters by ion-exchange method. Chemosphere 56 (2), 91–106.
- Dong, X., Wang, Y., Jia, M., Niu, Z., Cai, J., Yu, X., Ke, X., Yao, J., Zhang, X., 2019a. Sustainable and scalable in-situ synthesis of hydrochar-wrapped Ti₃AlC₂-derived nanofibers as adsorbents to remove heavy metals. Bioresour. Technol. 282, 222—227.
- Dong, Y., Sang, D., He, C., Sheng, X., Lei, L., 2019b. Mxene/alginate composites for lead and copper ion removal from aqueous solutions. RSC Adv. 9 (50), 29015–29022.
- Ertugay, N., Acar, F.N., 2014. The degradation of direct blue 71 by sono, photo and sonophotocatalytic oxidation in the presence of ZnO nanocatalyst. Appl. Surf. Sci. 318, 121–126
- Fard, A.K., McKay, G., Chamoun, R., Rhadfi, T., Preud'Homme, H., Atieh, M.A., 2017. Barium removal from synthetic natural and produced water using MXene as two dimensional (2-D) nanosheet adsorbent. Chem. Eng. J. 317, 331–342.
- Feng, A., Yu, Y., Wang, Y., Jiang, F., Yu, Y., Mi, L., Song, L., 2017. Two-dimensional MXene Ti₃C₂ produced by exfoliation of Ti₃AlC₂. Mater. Des. 114, 161–166.
- Fu, F., Wang, Q., 2011. Removal of heavy metal ions from wastewaters: a review. J. Environ. Manag. 92 (3), 407–418.
- Fu, F., Xie, L., Tang, B., Wang, Q., Jiang, S., 2012. Application of a novel strategy—advanced Fenton-chemical precipitation to the treatment of strong stability chelated heavy metal containing wastewater. Chem. Eng. J. 189–190, 283–287.
- Fu, L., Yan, Z., Zhao, Q., Yang, H., 2018. Novel 2D nanosheets with potential applications in heavy metal purification: a review. Adv. Mater. Interfaces 5 (23), 1801094.
- Gao, G., Ding, G., Li, J., Yao, K., Wu, M., Qian, M., 2016. Monolayer MXenes: promising half-metals and spin gapless semiconductors. Nanoscale 8 (16), 8986–8994.
- Ghidiu, M., Lukatskaya, M.R., Zhao, M.Q., Gogotsi, Y., Barsoum, M.W., 2014. Conductive two-dimensional titanium carbide 'clay' with high volumetric

- capacitance. Nature 516 (7529), 78-81.
- Giammar, D.E., Maus, C.I., Xie, L., 2007. Effects of particle size and crystalline phase on lead adsorption to titanium dioxide nanoparticles, Environ, Eng. Sci. 24 (1).
- Gong, R., Jin, Y., Chen, J., Hu, Y., Sun, J., 2007. Removal of basic dyes from aqueous solution by sorption on phosphoric acid modified rice straw. Dyes Pigments 73 (3), 332-337.
- Gu, P., Xing, J., Wen, T., Zhang, R., Wang, J., Zhao, G., Hayat, T., Ai, Y., Lin, Z., Wang, X., 2018 Experimental and theoretical calculation investigation on efficient Pb(II) adsorption on etched Ti₂AlC₂ nanofibers and nanosheets, Environ, Sci. Nano 5 (4), 946 - 955.
- Guo, J., Fu, H., Zou, G., Zhang, Q., Zhang, Z., Peng, Q., 2016a. Theoretical interpretation on lead adsorption behavior of new two-dimensional transition metal carbides and nitrides. J. Alloys Compd. 684, 504–509.
- Guo, J., Peng, Q., Fu, H., Zou, G., Zhang, Q., 2015. Heavy-metal adsorption behavior of two-dimensional alkalization-intercalated MXene by first-principles calculations, J. Phys. Chem. C 119 (36), 20923–20930. Guo, Z., Zhou, J., Zhu, L., Sun, Z., 2016b. MXene: a promising photocatalyst for water
- splitting, J. Mater. Chem. A 4 (29), 11446–11452. Halim, J., Lukatskaya, M.R., Cook, K.M., Lu, J., Smith, C.R., Naslund, L.A., May, S.J.,
- Hultman, L., Gogotsi, Y., Eklund, P., Barsoum, M.W., 2014. Transparent conductive two-dimensional titanium carbide epitaxial thin films. Chem. Mater. 26 (7), 2374-2381.
- Hong Ng, V.M., Huang, H., Zhou, K., Lee, P.S., Que, W., Xu, J.Z., Kong, L.B., 2017. Recent progress in layered transition metal carbides and/or nitrides (MXenes) and their composites: synthesis and applications. J. Mater. Chem. A 5 (7), 3039-3068
- Hu, Q., Sun, D., Wu, Q., Wang, H., Wang, L., Liu, B., Zhou, A., He, J., 2013. MXene: a new family of promising hydrogen storage medium. J. Phys. Chem. A 117 (51), 14253-14260.
- Huang, Z., Liu, B., Liu, J., 2019. Mn²⁺-assisted DNA oligonucleotide adsorption on Ti₂C MXene nanosheets. Langmuir 35 (30), 9858-9866.
- Jasper, J.T., Yang, Y., Hoffmann, M.R., 2017. Toxic byproduct formation during electrochemical treatment of latrine wastewater. Environ. Sci. Technol. 51 (12), 7111-7119
- Jun, B.-M., Heo, J., Taheri-Qazvini, N., Park, C.M., Yoon, Y., 2020a. Adsorption of selected dyes on Ti₃C₂T_x MXene and Al-based metal-organic framework. Ceram. Int. 46 (3), 2960-2968.
- Jun, B.-M., Her, N., Park, C.M., Yoon, Y., 2020b. Effective removal of Pb(II) from synthetic wastewater using Ti₃C₂T_x MXene. Environ. Sci. Water Res. Technol. 6 (1), 173–180.
- Jun, B.-M., Kim, S., Heo, J., Park, C.M., Her, N., Jang, M., Huang, Y., Han, J., Yoon, Y., 2018. Review of MXenes as new nanomaterials for energy storage/delivery and selected environmental applications. Nano Res 12 (3), 471-487.
- Karaçetin, G., Sivrikaya, S., Imamoğlu, M., 2014. Adsorption of methylene blue from aqueous solutions by activated carbon prepared from hazelnut husk using zinc chloride. J. Anal. Appl. Pyrolysis 110, 270-276.
- Khan, A.R., Husnain, S.M., Shahzad, F., Mujtaba-Ul-Hassan, S., Mehmood, M., Ahmad, J., Mehran, M.T., Rahman, S., 2019. Two-dimensional transition metal carbide (Ti₃C₂T_x) as an efficient adsorbent to remove cesium (Cs⁺). Dalton Trans. 48 (31), 11803-11812.
- Lei, J.-C., Zhang, X., Zhou, Z., 2015. Recent advances in MXene: preparation, properties, and applications. Front. Physiol. 10 (3), 276-286.
- Lei, Y., Cui, Y., Huang, Q., Dou, J., Gan, D., Deng, F., Liu, M., Li, X., Zhang, X., Wei, Y., 2019. Facile preparation of sulfonic groups functionalized Mxenes for efficient removal of methylene blue. Ceram. Int. 45 (14), 17653–17661.
- Li, K., Zou, G., Jiao, T., Xing, R., Zhang, L., Zhou, J., Zhang, Q., Peng, Q., 2018. Selfassembled MXene-based nanocomposites via layer-by-layer strategy for elevated adsorption capacities. Colloids Surf. A Physicochem. Eng. Asp. 553,
- Li, S., Wang, L., Peng, J., Zhai, M., Shi, W., 2019. Efficient thorium(IV) removal by twodimensional Ti₂CT_x MXene from aqueous solution. Chem. Eng. J. 366, 192–199.
- Lian, F., Sun, B., Chen, X., Zhu, L., Liu, Z., Xing, B., 2015. Effect of humic acid (HA) on sulfonamide sorption by biochars. Environ. Pollut. 204, 306-312.
- Lipatov, A., Alhabeb, M., Lukatskaya, M.R., Boson, A., Gogotsi, Y., Sinitskii, A., 2016. Effect of synthesis on quality, electronic properties and environmental stability of individual monolayer Ti₃C₂ MXene flakes. Adv. Electron. Mater. 2 (12),
- Liu, F., Zhou, A., Chen, J., Jia, J., Zhou, W., Wang, L., Hu, Q., 2017a. Preparation of Ti₃C₂ and Ti₂C MXenes by fluoride salts etching and methane adsorptive properties. Appl. Surf. Sci. 416, 781-789.
- Liu, F., Zhou, A., Chen, J., Zhang, H., Cao, J., Wang, L., Hu, Q., 2016. Preparation and methane adsorption of two-dimensional carbide Ti₂C. Adsorption 22 (7),
- Liu, G., Shen, J., Liu, Q., Liu, G., Xiong, J., Yang, J., Jin, W., 2018a. Ultrathin twodimensional MXene membrane for pervaporation desalination. J. Membr. Sci. 548, 548-558,
- Liu, L., Li, D., Li, C., Ji, R., Tian, X., 2018b. Metal nanoparticles by doping carbon nanotubes improved the sorption of perfluorooctanoic acid. J. Hazard Mater. 351, 206-214.
- Liu, L., Tan, S.J., Horikawa, T., Do, D.D., Nicholson, D., Liu, J., 2017b. Water adsorption on carbon - a review. Adv. Colloid Interface Sci. 250, 64-78.
- Lukatskaya, M.R., Mashtalir, O., Ren, C.E., Dall'Agnese, Y., Rozier, P., Taberna, P.L., Naguib, M., Simon, P., Barsoum, M.W., Gogotsi, Y., 2013. Cation intercalation and high volumetric capacitance of two-dimensional titanium carbide. Science 341

- (6153), 1502-1505.
- Ma, R., Sasaki, T., 2015. Two-dimensional oxide and hydroxide nanosheets: controllable high-quality exfoliation, molecular assembly, and exploration of functionality. Acc. Chem. Res. 48 (1), 136–143.
- Mashtalir, O., Cook, K.M., Mochalin, V.N., Crowe, M., Barsoum, M.W., Gogotsi, Y., 2014. Dye adsorption and decomposition on two-dimensional titanium carbide in aqueous media. J. Mater. Chem. A 2 (35), 14334–14338.
- Mashtalir, O., Lukatskaya, M.R., Zhao, M.Q., Barsoum, M.W., Gogotsi, Y., 2015. Amineassisted delamination of Nb₂C MXene for Li-ion energy storage devices. Adv. Mater, 27 (23), 3501-3506.
- Mashtalir, O., Naguib, M., Mochalin, V.N., Dall'Agnese, Y., Heon, M., Barsoum, M.W., Gogotsi, Y., 2013. Intercalation and delamination of layered carbides and carbonitrides, Nat. Commun. 4 (1), 1716.
- Meng, F., Seredych, M., Chen, C., Gura, V., Mikhalovsky, S., Sandeman, S., Ingavle, G., Ozulumba, T., Miao, L., Anasori, B., Gogotsi, Y., 2018. MXene sorbents for removal of urea from dialysate: a step toward the wearable artificial kidney. ACS Nano 12 (10), 10518-10528.
- Moghaddam, S.S., Moghaddam, M.R., Arami, M., 2010. Coagulation/flocculation process for dve removal using sludge from water treatment plant; optimization through response surface methodology. J. Hazard Mater. 175 (1–3), 651–657.
- Morales-García, Á., Fernández-Fernández, A., Viñes, F., Illas, F., 2018. CO₂ abatement using two-dimensional MXene carbides. J. Mater. Chem. A 6 (8), 3381–3385. Mu, W., Du, S., Li, X., Yu, Q., Wei, H., Yang, Y., Peng, S., 2019. Removal of radioactive
- palladium based on novel 2D titanium carbides. Chem. Eng. J. 358, 283-290.
- Mu, W., Du, S., Yu, Q., Li, X., Wei, H., Yang, Y., 2018. Improving barium ion adsorption on two-dimensional titanium carbide by surface modification. Dalton Trans. 47 (25), 8375-8381.
- Naguib, M., Come, J., Dyatkin, B., Presser, V., Taberna, P.-L., Simon, P., Barsoum, M.W., Gogotsi, Y., 2012a. MXene: a promising transition metal carbide anode for lithium-ion batteries. Electrochem. Commun. 16 (1), 61-64.
- Naguib, M., Gogotsi, Y., 2015. Synthesis of two-dimensional materials by selective extraction. Acc. Chem. Res. 48 (1), 128-135.
- Naguib, M., Kurtoglu, M., Presser, V., Lu, J., Niu, J., Heon, M., Hultman, L., Gogotsi, Y., Barsoum, M.W., 2011. Two-dimensional nanocrystals produced by exfoliation of Ti₃AlC₂. Adv. Mater. 23 (37), 4248-4253.
- Naguib, M., Mashtalir, O., Carle, J., Presser, V., Lu, J., Hultman, L., Gogotsi, Y., Barsoum, M.W., 2012b. Two-dimensional transition metal carbides. ACS Nano 6 (2) 1322-1331
- Naguib, M., Mochalin, V.N., Barsoum, M.W., Gogotsi, Y., 2014. 25th anniversary article: MXenes: a new family of two-dimensional materials. Adv. Mater. 26 (7), 992-1005
- Naguib, M., Unocic, R.R., Armstrong, B.L., Nanda, J., 2015. Large-scale delamination of multi-layers transition metal carbides and carbonitrides "MXenes. Dalton Trans. 44 (20), 9353-9358.
- Novoselov, K.S., Geim, A.K., Morozov, S.V., Jiang, D., Zhang, Y., Dubonos, S.V., Grigorieva, I.V., Firsov, A.A., 2004. Electric field effect in atomically thin carbon films. Science 306 (5696), 666-669.
- Oguz, E., Keskinler, B., 2005. Determination of adsorption capacity and thermodynamic parameters of the PAC used for bomaplex red CR-L dye removal. Colloids Surf. A Physicochem. Eng. Asp. 268 (1-3), 124-130.
- Peng, Q., Guo, J., Zhang, Q., Xiang, J., Liu, B., Zhou, A., Liu, R., Tian, Y., 2014. Unique lead adsorption behavior of activated hydroxyl group in two-dimensional titanium carbide. J. Am. Chem. Soc. 136 (11), 4113-4116.
- Rasool, K., Mahmoud, K.A., Johnson, D.J., Helal, M., Berdiyorov, G.R., Gogotsi, Y., 2017. Efficient antibacterial membrane based on two-dimensional Ti₃C₂T_x (MXene) nanosheets. Sci. Rep. 7 (1), 1-11.
- Rasool, K., Pandey, R.P., Rasheed, P.A., Buczek, S., Gogotsi, Y., Mahmoud, K.A., 2019. Water treatment and environmental remediation applications of twodimensional metal carbides (MXenes). Mater. Today 30, 80-102.
- Rozmysłowska-Wojciechowska, A., Wojciechowski, T., Ziemkowska, W., Chlubny, L., Olszyna, A., Jastrzębska, A.M., 2019. Surface interactions between 2D Ti₃C₂/Ti₂C MXenes and lysozyme. Appl. Surf. Sci. 473, 409-418.
- Sakthivel, S., Neppolian, B., Shankar, M.V., Arabindoo, B., Palanichamy, M., Murugesan, V., 2003. Solar photocatalytic degradation of azo dye: comparison of photocatalytic efficiency of ZnO and TiO2. Sol. Energy Mater. Sol. Cells 77 (1),
- Sarycheva, A., Polemi, A., Liu, Y., Dandekar, K., Anasori, B., Gogotsi, Y., 2018. 2D titanium carbide (MXene) for wireless communication. Sci. Adv. 4 (9), eaau0920.
- Shahzad, A., Nawaz, M., Moztahida, M., Jang, J., Tahir, K., Kim, J., Lim, Y., Vassiliadis, V.S., Woo, S.H., Lee, D.S., 2019a. Ti₃C₂T_x MXene core-shell spheres for ultrahigh removal of mercuric ions. Chem. Eng. J. 368, 400-408.
- Shahzad, A., Nawaz, M., Moztahida, M., Tahir, K., Kim, J., Lim, Y., Kim, B., Jang, J., Lee, D.S., 2019b. Exfoliation of titanium aluminum carbide (211 MAX phase) to form nanofibers and two-dimensional nanosheets and their application in aqueous-phase cadmium sequestration. ACS Appl. Mater. Interfaces 11 (21), 19156-19166.
- Shahzad, A., Rasool, K., Miran, W., Nawaz, M., Jang, J., Mahmoud, K.A., Lee, D.S., 2018. Mercuric ion capturing by recoverable titanium carbide magnetic nanocomposite. J. Hazard Mater. 344, 811-818.
- Shahzad, A., Rasool, K., Miran, W., Nawaz, M., Jang, J., Mahmoud, K.A., Lee, D.S., 2017. Two-dimensional Ti₃C₂T_x MXene nanosheets for efficient copper removal from water. ACS Sustain. Chem. Eng. 5 (12), 11481-11488.
- Tan, K.B., Vakili, M., Horri, B.A., Poh, P.E., Abdullah, A.Z., Salamatinia, B., 2015. Adsorption of dyes by nanomaterials: recent developments and adsorption mechanisms. Separ. Purif. Technol. 150, 229-242.

- Tang, H., Feng, H., Wang, H., Wan, X., Liang, J., Chen, Y., 2019. Highly conducting MXene-silver nanowire transparent electrodes for flexible organic solar cells. ACS Appl. Mater. Interfaces 11 (28), 25330–25337.
- Tang, Y., Yang, C., Que, W., 2018. A novel two-dimensional accordion-like titanium carbide (MXene) for adsorption of Cr(VI) from aqueous solution. J. Adv. Dielectr. 8, 1850035, 05.
- Wang, G., Wang, X., Chai, X., Liu, J., Deng, N., 2010a. Adsorption of uranium (VI) from aqueous solution on calcined and acid-activated kaolin. Appl. Clay Sci. 47 (3–4), 448–451.
- Wang, L., Song, H., Yuan, L., Li, Z., Zhang, P., Gibson, J.K., Zheng, L., Wang, H., Chai, Z., Shi, W., 2019. Effective removal of anionic Re(VII) by surface-modified Ti₂CT_X MXene nanocomposites: implications for Tc(VII) sequestration. Environ. Sci. Technol. 53 (7), 3739–3747.
- Wang, L., Song, H., Yuan, L., Li, Z., Zhang, Y., Gibson, J.K., Zheng, L., Chai, Z., Shi, W., 2018. Efficient U(VI) reduction and sequestration by Ti₂CT_x MXene. Environ. Sci. Technol. 52 (18), 10748–10756.
- Wang, L., Tao, W., Yuan, L., Liu, Z., Huang, Q., Chai, Z., Gibson, J.K., Shi, W., 2017a. Rational control of the interlayer space inside two-dimensional titanium carbides for highly efficient uranium removal and imprisonment. Chem. Commun. 53 (89), 12084–12087.
- Wang, L., Yuan, L., Chen, K., Zhang, Y., Deng, Q., Du, S., Huang, Q., Zheng, L., Zhang, J., Chai, Z., Barsoum, M.W., Wang, X., Shi, W., 2016. Loading actinides in multi-layered structures for nuclear waste treatment: the first case study of uranium capture with vanadium carbide MXene. ACS Appl. Mater. Interfaces 8 (25), 16396—16403.
- Wang, N., Zhu, L., Wang, M., Wang, D., Tang, H., 2010b. Sono-enhanced degradation of dye pollutants with the use of H_2O_2 activated by Fe_3O_4 magnetic nanoparticles as peroxidase mimetic. Ultrason. Sonochem. 17 (1), 78–83.
- Wang, X., Garnero, C., Rochard, G., Magne, D., Morisset, S., Hurand, S., Chartier, P., Rousseau, J., Cabioc'h, T., Coutanceau, C., Mauchamp, V., Célérier, S., 2017b. A new etching environment (FeF₃/HCl) for the synthesis of two-dimensional titanium carbide MXenes: a route towards selective reactivity vs. water. J. Mater. Chem. A 5 (41), 22012–22023.
- Wei, Z., Peigen, Z., Wubian, T., Xia, Q., Yamei, Z., ZhengMing, S., 2018. Alkali treated Ti₃C₂T_x MXenes and their dye adsorption performance. Mater. Chem. Phys. 206, 270–276.
- Wu, Y., Pang, H., Liu, Y., Wang, X., Yu, S., Fu, D., Chen, J., Wang, X., 2019. Environmental remediation of heavy metal ions by novel-nanomaterials: a review. Environ. Pollut. 246, 608–620.
- Xie, X., Xue, Y., Li, L., Chen, S., Nie, Y., Ding, W., Wei, Z., 2014. Surface Al leached Ti₂AlC₂ as a substitute for carbon for use as a catalyst support in a harsh corrosive electrochemical system. Nanoscale 6 (19), 11035—11040.
- Xu, D., Zhou, X., Wang, X., 2008. Adsorption and desorption of Ni²⁺ on Namontmorillonite: effect of pH, ionic strength, fulvic acid, humic acid and addition sequences. Appl. Clay Sci. 39 (3-4), 133-141.
- Yang, X., Wan, Y., Zheng, Y., He, F., Yu, Z., Huang, J., Wang, H., Ok, Y.S., Jiang, Y., Gao, B., 2019. Surface functional groups of carbon-based adsorbents and their

- roles in the removal of heavy metals from aqueous solutions: a critical review. Chem. Eng. J. 366, 608–621.
- Ying, Y., Liu, Y., Wang, X., Mao, Y., Cao, W., Hu, P., Peng, X., 2015. Two-dimensional titanium carbide for efficiently reductive removal of highly toxic chromium(VI) from water. ACS Appl. Mater. Interfaces 7 (3), 1795—1803.
- Zhang, P., Wang, L., Yuan, L.-Y., Lan, J.-H., Chai, Z.-F., Shi, W.-Q., 2019a. Sorption of Eu(III) on MXene-derived titanate structures: the effect of nano-confined space. Chem. Eng. J. 370, 1200–1209.
- Zhang, P., Xiang, M., Liu, H., Yang, C., Deng, S., 2019b. Novel two-dimensional magnetic titanium carbide for methylene blue removal over a wide pH range: insight into removal performance and mechanism. ACS Appl. Mater. Interfaces 11 (27), 24027–24036.
- Zhang, X., Wang, H., Hu, R., Huang, C., Zhong, W., Pan, L., Feng, Y., Qiu, T., Zhang, C., Yang, J., 2019c. Novel solvothermal preparation and enhanced microwave absorption properties of Ti₃C₂T_x MXene modified by in situ coated Fe₃O₄ nanoparticles. Appl. Surf. Sci. 484, 383–391.
- Zhang, Y.-J., Zhou, Z.-J., Lan, J.-H., Ge, C.-C., Chai, Z.-F., Zhang, P., Shi, W.-Q., 2017. Theoretical insights into the uranyl adsorption behavior on vanadium carbide MXene. Appl. Surf. Sci. 426, 572–578.
- Zhang, Y., Wang, L., Zhang, N., Zhou, Z., 2018. Adsorptive environmental applications of MXene nanomaterials: a review. RSC Adv. 8 (36), 19895–19905. Zhang, Y.J., Lan, J.H., Wang, L., Wu, Q.Y., Wang, C.Z., Bo, T., Chai, Z.F., Shi, W.Q., 2016.
- Zhang, Y.J., Lan, J.H., Wang, L., Wu, Q.Y., Wang, C.Z., Bo, T., Chai, Z.F., Shi, W.Q., 2016. Adsorption of uranyl species on hydroxylated titanium carbide nanosheet: a first-principles study. J. Hazard Mater. 308, 402-410.
- Zhao, G., Ren, X., Gao, X., Tan, X., Li, J., Chen, C., Huang, Y., Wang, X., 2011. Removal of Pb (II) ions from aqueous solutions on few-layered graphene oxide nanosheets. Dalton Trans. 40 (41), 10945–10952.
- Zhou, J., Lü, Q.-F., Luo, J.-J., 2017. Efficient removal of organic dyes from aqueous solution by rapid adsorption onto polypyrrole—based composites. J. Clean. Prod. 167. 739—748.
- Zhu, H.-Y., Jiang, R., Xiao, L., 2010. Adsorption of an anionic azo dye by chitosan/ kaolin/ γ -Fe₂O₃ composites. Appl. Clay Sci. 48 (3), 522–526.
- Zhu, M., Huang, Y., Deng, Q., Zhou, J., Pei, Z., Xue, Q., Huang, Y., Wang, Z., Li, H., Huang, Q., 2016. Highly flexible, freestanding supercapacitor electrode with enhanced performance obtained by hybridizing polypyrrole chains with MXene. Adv. Energy Mater. 6 (21), 1600969.
- Zhu, X., Liu, B., Hou, H., Huang, Z., Zeinu, K.M., Huang, L., Yuan, X., Guo, D., Hu, J., Yang, J., 2017. Alkaline intercalation of Ti₃C₂ MXene for simultaneous electrochemical detection of Cd(II), Pb(II), Cu(II) and Hg(II). Electrochim. Acta 248, 46–57.
- Zhu, Z., Xiang, M., Shan, L., He, T., Zhang, P., 2019. Effect of temperature on methylene blue removal with novel 2D-Magnetism titanium carbide. J. Solid State Chem. 280, 120989.
- Zou, G., Guo, J., Peng, Q., Zhou, A., Zhang, Q., Liu, B., 2016. Synthesis of urchin-like rutile titania carbon nanocomposites by iron-facilitated phase transformation of MXene for environmental remediation. J. Mater. Chem. A 4 (2), 489–499.